Evolutionary Systematics. 8 2024, 199–218 | DOI 10.3897/evolsyst.8.126393

PENSOFT

EVOLUTIONARY SYSTEMATICS

Top mountain areas of subtropical southern Brazil sheltering four new small-ranged catfishes (Siluriformes, Trichomycteridae): relationships and taxonomy

Wilson J. E. M. Costa[1], Caio R. M. Feltrin[1], José Leonardo O. Mattos[1], Axel M. Katz[1]

1 *Laboratory of Systematics and Evolution of Teleost Fishes, Institute of Biology, Federal University of Rio de Janeiro, Caixa Postal 68049, CEP 21941-971, Rio de Janeiro, Brazil*

https://zoobank.org/973DECB5-340A-41CE-9AEE-B968664489B2

Corresponding author: Wilson J. E. M. Costa (wcosta@acd.ufrj.br)

Academic editor: Oliver Hawlitschek ♦ **Received** 28 April 2024 ♦ **Accepted** 12 August 2024 ♦ **Published** 11 September 2024

Abstract

Mountainous regions typically host a great diversity of small-ranged species, often contributing for delineating world biodiversity hotspots. Species of trichomycterine catfishes have been recorded for several high-altitude areas of tropical South America, but field inventories in top mountains of southern Brazil are still rare. Here we report four new small-ranged species collected in streams of the Rio Iguaçu at Serra do Espigão (RISE) in altitudes between about 970 and 1020 m asl, one in the eastern portion of RISE and three in the western portion. A molecular phylogenetic analysis indicated that these species belong to the *Cambeva* beta-clade, which comprises all species endemic to the Rio Iguaçu drainage, but together not forming a monophyletic group. The analysis also indicated that species endemic to high altitudes are variably related to species from lower altitudes. The only eastern RISE species appears in a basal position of a well-supported clade (*Cambeva* beta1-clade), with the western RISE species appearing in a subclade of the *Cambeva* beta1-clade with species occurring in a vast area of southern Brazil. New species are diagnosed by combinations of morphological character states, including meristic, colouration, latero-sensory system, and osteological data.

Key Words

Cambeva, Molecular phylogeny, Mountain biodiversity, Rio Iguaçu drainage, Serra do Espigão

Introduction

Mountainous areas of tropical and subtropical regions of the world host a great biodiversity, commonly concentrating numerous small-ranged species (Rahbek et al. 2007, 2019) and contributing for delineation of the most important biodiversity hotspots (Myers et al. 2000). Among fish groups, Trichomycterinae (hereafter trichomycterines) is the most diverse in South American river mountains (e.g. Costa et al. 2021), with species being sporadically recorded from high altitude localities of Andes since the 18th century (e.g. Valenciennes 1832) until the 20th one (e.g. Arratia and Menu Marque 1984). Recent studies, however, have consistently recorded the occurrence of numerous new trichomycterines from various Andean regions with geographic distribution restricted to small areas in altitudes between around 1,200 and 4,000 m asl (e.g. Fernández and Schaefer 2003; DoNascimiento et al. 2014; Fernández and Liota 2016; Fernández et al. 2023). Species occurring in high Andean areas are often confined to particular environments such as caves (e.g. Castellanos-Morales 2008, 2018; Mesa et al. 2018), phreatic waters (e.g. Fernández and de Pinna 2005) and thermal water wells (Fernandéz and Vari 2012). On the other hand, in the mountain ranges of subtropical southern Brazil, where higher altitudes barely surpass 1800 m asl, recent studies also have revealed some small-ranged species of *Cambeva* Katz, Barbosa, Mattos & Costa, 2018 only found at altitudes above 900 m asl (e.g. Ferrer and Malabarba

2011; Costa et al. 2021, 2023a), but field inventories at higher areas of this region are still rare and many sites remain unsampled.

With a surface area of about 72,600 km2, the Rio Iguaçu drainage, a main tributary of the Rio Paraná basin, is situated in a region characterized by a sequence of mountain ranges and plateaus (i.e. Serra da Esperança, Serra do Espigão, Serra do Mar; e.g. Ab'Saber 2007). This landscape contains extensive areas of rapids and waterfalls inhabited by a remarkable diversity of species of *Cambeva*, with a great concentration reported for some areas. For example, Wosiacki and collaborators described six species and reported the occurrence of other two already described species from the Rio Jordão, a tributary of the middle Rio Iguaçu (Wosiacki and Garavello 2004; Wosiacki and de Pinna 2008a, b). A total of 13 nominal species have been recorded for this drainage (Haseman 1911; Miranda Ribeiro 1968; de Pinna 1992; Wosiacki and Garavello 2004; Wosiacki and de Pinna 2008a, b; dos Reis et al. 2021, 2023; Costa et al. 2022) and phylogenetic studies have indicated that all species belong to a single large intrageneric clade, called *Cambeva* beta-clade (Costa et al. 2023b). However, all records of *Cambeva* for the Rio Iguaçu drainage are concentrated in the northern part of the drainage, with no data available about its occurrence in the southern part of the drainage, where rivers and streams drain the Serra do Espigão, which is part of a long chain of mountain ranges that stretches across southern Brazil under the name Serra Geral. The section known as Serra do Espigão forms a long plateau running east-west, with higher average altitudes between 900 and 1200 m, having its eastern portion in contact with the coastal mountain range chain called Serra do Mar.

A great diversity of species of *Cambeva* was found during a detailed recent field inventory (March/April 2023) in rivers and streams of an area about 9,000 km^2 belonging to the Rio Iguaçu drainage at Serra do Espigão (hereafter RISE) by one of us (CRMF). Most of these species were found in about 25 localities of a broad area at altitudes below about 840 m asl and were conspecific or morphologically similar to species widely distributed in other parts of the drainage (i. e. *Cambeva naipi* (Wosiacki & Garavello, 2004), *Cambeva papillifera* (Wosiacki & Garavello, 2004), *Cambeva stawiarski* (Miranda Ribeiro, 1968) or occurring in adjacent coastal basins to the east (i.e. *C. barbosae* Costa, Feltrin & Katz, 2021). Contrastingly, four undescribed species were found in isolated points of RISE at altitudes between about 970 and 1020 m asl, one of them in the eastern portion of RISE, and three in neighbouring drainages at the western portion. All these species were found only in small areas, despite sampling efforts at various points in different altitudes of their sub-drainages. Furthermore, they were rare in their habitats, making necessary a second collecting trip (June/July 2023) to supplement the material necessary for adequate descriptions. The objectives of the present study are to perform a molecular phylogenetic analysis to positioning the new species among the main intrageneric lineages and to describe the four new species.

Materials and methods

Specimens

Specimens were captured using dip nets during daylight. Collecting permits were provided by ICMBio (Instituto Chico Mendes de Conservação da Biodiversidade; permit number: 38553-13). Methods for collections were approved by CEUA-CCS-UFRJ (Ethics Committee for Animal Use of Federal University of Rio de Janeiro; permit numbers: 065/18 and 084/23). Fixation and preservation of specimens as described in Costa et al. (2023b). Osteological preparations followed Taylor and Van Dyke (1985). Specimens were deposited in Instituto de Biologia, Universidade Federal do Rio de Janeiro (UFRJ) and Centro de Ciências Agrárias e Ambientais, Universidade Federal do Maranhão (CICCAA). Abbreviations used in list of specimens are: C&S, cleared and stained specimens for osteological examination; SL, standard length. In localities where specimens were collected, geographical names are according to Portuguese names used in the region. Comparative material is listed in our previous studies on the genus *Cambeva* (Costa et al. 2023a, b and included references).

Morphological data

Measurements were according to landmarks described in Costa (1992), modified in Costa et al. (2020a) and were made in well-preserved specimens above about 40 mm SL. Meristic data and fin ray formulae followed Costa et al. (2020a) based on Costa (1992) and Bockmann and Sazima (2004). Osteological morphology was primarily approached using a stereomicroscope Zeiss Stemi SV 6 with camera lucida. Terminology for osteological structures is according to Costa (2021), with more recent updates described in Kubicek (2022). Nomenclature for pores of the latero-sensory system followed Arratia and Huaquin (1995), except for post-orbital pores as proposed by Bockmann and Sazima (2004).

DNA extraction, amplification and sequencing

DNA extraction, amplification and sequencing followed the same methods as described in our recent phylogenetic studies on *Cambeva* (e.g. Costa et al. 2023b), using the same markers: the mitochondrially encoded genes cytochrome b (CYTB) and cytochrome c oxidase I (COX1) and the nuclear encoded gene recombination activating 2 (RAG2). We used the following primers: Cytb Siluri F and Cytb Siluri R (Villa-Verde et al. 2012), CatThr29 and Glu 31 (Unmack et al. 2009), and Glu 5 and Cb23 (Barros et al. 2015) for CYTB; FISHF1 and FISHR1 (Ward et al. 2005) for COX1; MHRAG2-F1 and MHRAG2-R1 (Hardman and Page 2003), RAG2 TRICHO F and RAG2 TRICHO R (Costa et al. 2020b), and RAG2 MCF and RAG2 MCR (Cramer et al. 2011) for RAG2. PCR reaction parameters

are those described in Costa et al. (2023b). Reading and interpretation of sequencing chromatograms and sequence edition were performed using MEGA 11 (Tamura et al. 2021). GenBank accession numbers appear in Table 1.

Phylogenetic analyses

Terminal taxa comprised the four new species and other 19 species of the *Cambeva* beta-clade, besides 13 congeners of other lineages and five outgroup species belonging to other trichomycterid lineages. The analysis comprised both DNA sequences here generated and those taken from our previous studies (Katz et al. 2018; Costa et al. 2023a, b) and from GenBank, first published in Ochoa et al. (2017a, 2017b) and Donin et al. (2022). The concatenated molecular data matrix comprised 2469 bp (COX1 685 bp, CYTB 993 bp, RAG2 791 bp). Each gene data set was individually aligned using the Clustal W algorithm (Chenna et al. 2003) implemented n MEGA 11. No stop codons and gaps were found. PartitionFinder2.1.1 (Lanfear et al. 2016) algorithm was used to calculate best-fit evolutive model schemes (Table 2), under the Corrected Akaike Information Criterion. Phylogenetic analyses were conducted using Bayesian Inference (BI) and Maximum Likelihood (ML) approaches. BI was performed in Beast 1.10.4 (Suchard at al. 2018), using two independent Markov Chain Monte Carlo (MCMC) runs with 3×10^7 generations, with sampling frequency of 1000 generation, using Tracer 1.7.2 (Rambaut et al. 2018) to verify convergence of the MCMC chains and the proper burn-in value. LogCombiner v.1.10.4 (Suchard et al. 2018) and Tree Annotator version 1.10.4 (Suchard et al. 2018) were used to combine and calculate the consensus tree, apply the 25% burn-in, and annotate the Bayesian posterior probabilities. ML was performed using IQTREE 2.2.0 (Minh et al. 2020), with node support evaluated by ultrafast bootstrap (UFBoot) (Hoang et al. 2018) and the Shimodaira-Hasegawa-like approximate likelihood ratio test (SH-aLRT), each using 1000 replicates.

Table 1. Terminal taxa, and GenBank accessions numbers by gene used in molecular analysis. Asterisks (*) indicate the newly added sequences.

	COI	CYTB	RAG2
Trichogenes longipinnis	OQ810037	MK123704	MF431117
Listrura tetraradiata	JQ231083	JQ231088.1	MN385826.1
Ituglanis boitata	OQ810038	MK123706	MK123758
Trichomycterus itatiayae	MW671552	MW679291	OL779233
Scleronema minutum	MK123685	MK123707	MK123759.1
Cambeva variegata	PP319019	PP328534	PP333217
Cambeva zonata	KY857986	KY858053	–
Cambeva brachykechenos	MN995669	MN995758	–
Cambeva diatropoporos	KY857996	KY858065	KY858213
Cambeva stawiarski	MN995720	MN995779	–
Cambeva perkos	KY857981	KY858050	–
Cambeva poikilos	KY857995	KY858064	–
Cambeva guaraquessaba	MN995662	MN995749	–
Cambeva naipi	MN995699	MN995771	–
Cambeva taroba	MN995708	MN995757	–
Cambeva tupinamba	MN995656	MN995751	–
Cambeva tropeira	MN995674	MN995752	–
Cambeva grisea	MN995671	MN995760	–
Cambeva imaruhy	MN995700	MN995766	OQ814191
Cambeva orbitofrontalis	MN995703	MN995764	OQ814192
Cambeva cubataonis	OQ095914	OQ110814	OQ110815
Cambeva iheringi	GU701893	KY858074	KY858223
Cambeva barbosae	MK123689.1	OQ110808	OQ110815.1
Cambeva diabola	JN989258	OQ110812	–
Cambeva balios	OQ810040	OQ814186	OQ814193
Cambeva chrysornata	MN995726	OQ110810	OQ110819
Cambeva pascuali	MF034463	OQ110811	OQ110820
Cambeva guaratuba	MN995721	MN995792	–
Cambeva panthera	OQ810041	OQ814187	OQ814194
Cambeva flavopicta	OQ810042	OQ814188	OQ814195
Cambeva podostemophila	OQ810043	OQ814189	OQ814196
Cambeva tourensis	MN995697	OQ814190	OQ814197 13283
Cambeva davisi	KR140345	MK123714	MK123762
Cambeva luteoreticulata	PP448186 *	PP449083 *	PP449087 *
Cambeva atrobrunnea	PP448187 *	PP449084 *	PP449088 *
Cambeva rotundipinna	PP448188 *	PP449085 *	PP449089 *
Cambeva galactica	PP448189 *	PP449086 *	PP449090 *
Cambeva biseriata	PP448190 *	OQ110806	OQ110817
Cambeva ventropapilata	PP448191 *	OQ110807	OQ110818
Cambeva guareiensis	PP448192 *	OQ110813	OQ110821
Cambeva castroi	–	MK123712	OQ110816

Table 2. Optimal partition schemes with their respective quantities of base pairs and the best-fitting evolutive models.

Partition	Base pairs	Evolutive Model
COI 1st	229	GTR+G
COI 2nd	228	TRN+G
COI 3rd	228	HKY+I
CYTB 1st	331	TRNEF+I+G
CYTB 2nd	331	HKY+I+G
CYTB 3rd	331	TRN+G
RAG2 2nd, 3rd	527	GTR+I
RAG2 1st	263	K80+I

New species diagnoses

Species here described were primarily diagnosed using unique morphological character states (i.e. not occurring in all other species of *Cambeva*), followed by unique combinations of morphological character states (see Davis and Nixon 1992). Morphological diagnoses were followed by molecular diagnoses based on the partial sequences of the mitochondrial genes COX1 and CYTB used the phylogenetic analysis (see above), following Costa et al. (2014) and Aguiar et al. (2022), using PAUP* 4 (Swofford 2002) to track base pair transformations. The position of each base pair relative to the entire gene was estimated by aligning the fragments with the nearly complete mitochondrial DNA genome of *Trichomycterus areolatus* Valenciennes, 1846 (accession number AP012026). In addition, although genetic distances alone are not informative to delimit species (e.g. DeSalle et al. 2005), we provided pairwise COX1 genetic distances between each new species and other species of the *Cambeva* beta-clade, calculated using the Kimura 2-parameter (Kimura 1980) model algorithm, implemented in MEGA 11, to illustrate interspecific ranges, indicating taxa with shortest distances).

Results

Phylogenetic relationships and comparative morphology

Both analyses generated similar topologies (Fig. 1), in which the *Cambeva* beta-clade is corroborated, including *Cambeva naipi* Wosiacki & Garavello, 2004 as the sister group to all other species. All the four RISE species are corroborated as members of the *Cambeva* beta-clade, but appearing in different sections of the tree, with the western RISE species (*C. galactica* Costa, Feltrin & Katz, sp. nov.) supported as a basal species of an inclusive

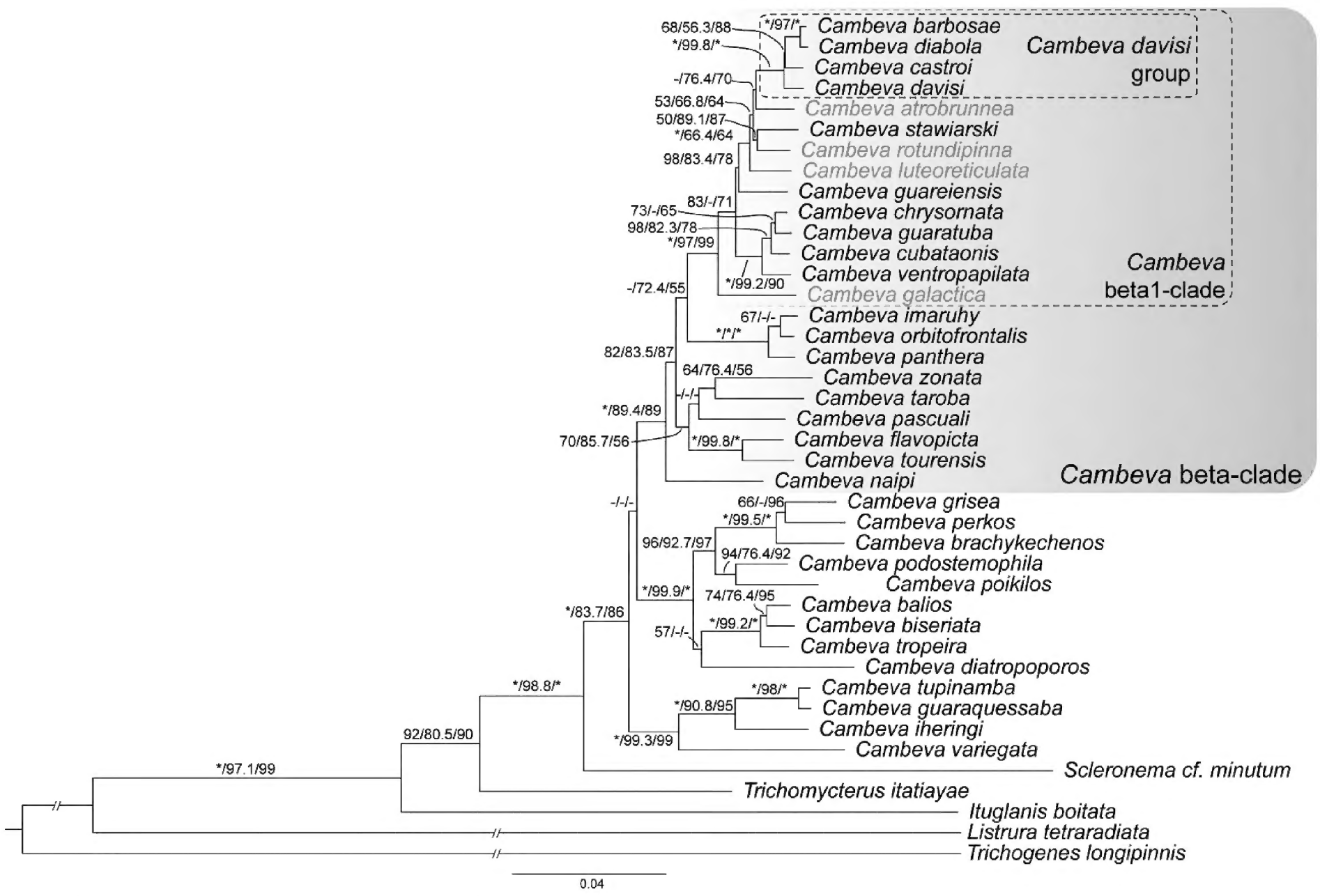

Figure 1. Bayesian phylogenetic tree obtained by BEAST for 36 species of *Cambeva* species and five outgroups, using three genes (COI, CYTB, and RAG2; total of 2469 bp). Species in red are the new species herein described. Numbers separated by bars (/) above branches indicate posterior probabilities from the Bayesian Inference, and ultrafast bootstrap (UFBoot) and the Shimodaira-Hasegawa-like approximate likelihood ratio test (SH-aLRT) from the Maximum Likelihood analysis inferred in IQTREE2. Asterisks (*) indicate maximum support values, and dashes (-) indicate support values below 50.

well-supported clade (hereafter *Cambeva* beta-1 clade) that also includes the three other RISE species. The three eastern RISE species are positioned in a subclade that also includes other species endemic to the Rio Iguaçu drainage (*Cambeva castroi* (Pinna, 1992), *Cambeva davisi* (Haseman, 1911), *Cambeva stawiarski* (Miranda Ribeiro, 1968)), as well as species that occur in adjacent coastal areas (*Cambeva barbosae* Costa, Feltrin & Katz, 2020) or in other drainages of the Paraná River basin (*Cambeva diabola* (Bockmann, Casatti & de Pinna, 2004), *Cambeva guareiensis* Katz & Costa, 2020). The analyses indicated that three western RISE species do not form a monophyletic group, but their position was weakly supported. In spite of a superficial similarity in their external morphology, the osteological analysis revealed a highly divergent bone morphology (see descriptions below), suggesting that they are not close relatives.

Taxonomic accounts

The four species here described share several morphological character states of the external morphology that are common among congeners of the beta-clade. In order to avoid unnecessarily repeating the same characteristics in each individual species description, below is a general description of character states shared by all four species.

General description of species from RISE

Body moderately slender, subcylindrical in anterior region, compressed in posterior region. Greatest body depth in area midway between pectoral-fin and pelvic-fin bases. Dorsal and ventral profile slightly convex between snout and dorsal-fin origin, about straight along caudal peduncle. Anus and urogenital papilla at vertical through middle part of dorsal-fin base or immediately posterior to it. Head sub-trapezoidal in dorsal view. Anterior profile of snout slightly convex in dorsal view. Eye small, dorsally positioned on head, in its anterior half. Distance between anterior and posterior nostrils shorter than distance between posterior nostril and orbit. Minute skin papillae on head surface. Mouth subterminal.

Supraorbital sensory canal continuous, posteriorly connected to posterior section of infraorbital canal, with three pores: s1, adjacent to medial margin of anterior nostril; s3, adjacent and just posterior to medial margin of posterior nostril; s6, in transverse line through posterior half of orbit. Pore s6 nearer orbit than its paired homologous pore. Posterior infraorbital sensory canal with two pores: pore i10, adjacent to ventral margin of orbit, and pore i11, posterior to orbit. Postorbital canal with two pores: po1, at vertical through posterior portion of interopercular patch of odontodes, and po2, at vertical through posterior portion of opercular patch of odontodes. Lateral line with two pores situated above and slightly posterior to pectoral-fin base.

Eastern RISE species

Cambeva galactica Costa, Feltrin & Katz, sp. nov.

https://zoobank.org/D7C5FF3B-FE1F-4F06-A8E4-B3F0D1ABF829

Figs 2, 3, 4A–C, Table 3

Type material. ***Holotype.*** Brazil • 1 ex., 76.9 mm SL; Santa Catarina State: Rio Negrinho Municipality: village of Volta Grande: stream tributary of Rio Preto, itself a tributary of Rio Negro, Rio Iguaçu drainage, Rio Paraná basin; 26°33'04"S, 49°40'14"W; about 970 m asl; 29 Mar. 2023; C.R.M. Feltrin, leg.; UFRJ 14064.

Paratypes. Brazil • 4 ex., 18.7–40.6 mm SL; same data as for holotype; UFRJ 13516. • 3 ex. (C&S), 40.5–64.9 mm SL; same data as for holotype; UFRJ 14065. • 2 ex. (DNA), 16.5–38.8 mm SL; same data as for holotype; UFRJ 13517. • 5 ex., 28.8–108.0 mm SL; same locality and collector as holotype; 28 Jun. 2023; UFRJ 13847.

Diagnosis. *Cambeva galactica* is distinguished from all congeners by a unique colour pattern in adult specimens consisting of flank and dorsum with longitudinal rows of interconnected yellowish white vermiculate diffuse marks (vs. never a similar colour pattern), and the presence of a distinctive projection on the anterior portion of the medial margin of the sesamoid supraorbital, connected by thin ligamentous tissue to a dorsal projection on the articulatory shell of the autopalatine for the lateral ethmoid (Fig. 4A; vs. never a similar process connected to that articulation). *Cambeva galactica* is also distinguished from all other species of the *Cambeva* beta-clade, except *Cambeva flavopicta* Costa, Feltrin & Katz, 2020, *Cambeva naipi* (Wosiacki & Garavello, 2004), *Cambeva taroba* (Wosiacki & Garavello, 2004), and *Cambeva tourense* Costa, Feltrin & Katz, 2023 by having six pectoral-fin rays (vs. five, seven, or eight). *Cambeva galactica* is distinguished from *C. flavopicta* and *C. tourense* by having well-developed pelvic fins (vs. absent); from *C. naipi* and *C. taroba* by having more interopercular odontodes 29–32 vs. 11 or 12 in *C. naipi* and 17–21 in *C. taroba*) and more jaw teeth (41–43 on the premaxilla and 39–46 on the dentary, vs. 25–34 and 23–32, respectively); from *C. naipi* by having 14 or 15 ribs (vs. 12 or 13), fewer opercular odontodes (eight or nine vs 12 or 13), and from *C. taroba* by having a minute pectoral-fin filament, its length less than 5% of the pectoral-fin length (vs. about 20%), fewer procurrent caudal-fin rays (18 or 19 dorsal and 12 or 13 ventral, vs. 26 or 27 and 21–23, respectively), more vertebrae (39 or 40 vs 36). Molecular diagnosis: 34 nucleotide substitutions, nine of them unique among taxa analysed*, and five unique for the *Cambeva* beta-clade **: COX1 103 (T→C)**, COX1 103 (G→A), COX1 117 (A→T)*, COX1 243 (A→G)*, COX1 309 (G→A), COX1 312 (C→A), COX1 321 (C→A), COX1 330 (C→A)*, COX1 483 (T→C), COX1 540 (A→G), COX1 547 (C→T), COX1 684 (A→C)*, CYTB 195 (T→C), CYTB 219 (T→C), CYTB 282 (C→T)**, CYTB 283 (T→C), CYTB 339 (C→T), COX1 342 (C→T), CYTB 394 (C→T), CYTB 399 (T→C)**, CYTB 495 (G→A),

Figure 2. *Cambeva galactica* Costa, Feltrin & Katz, sp. nov., holotype, UFRJ 14064, 76.9 mm SL. **A.** Lateral view; **B.** Dorsal view; **C.** Ventral view.

Figure 3. *Cambeva galactica* Costa, Feltrin & Katz, sp. nov., paratype, UFRJ 13847, 33.4 mm SL. **A.** Lateral view; **B.** Dorsal view; **C.** Ventral view.

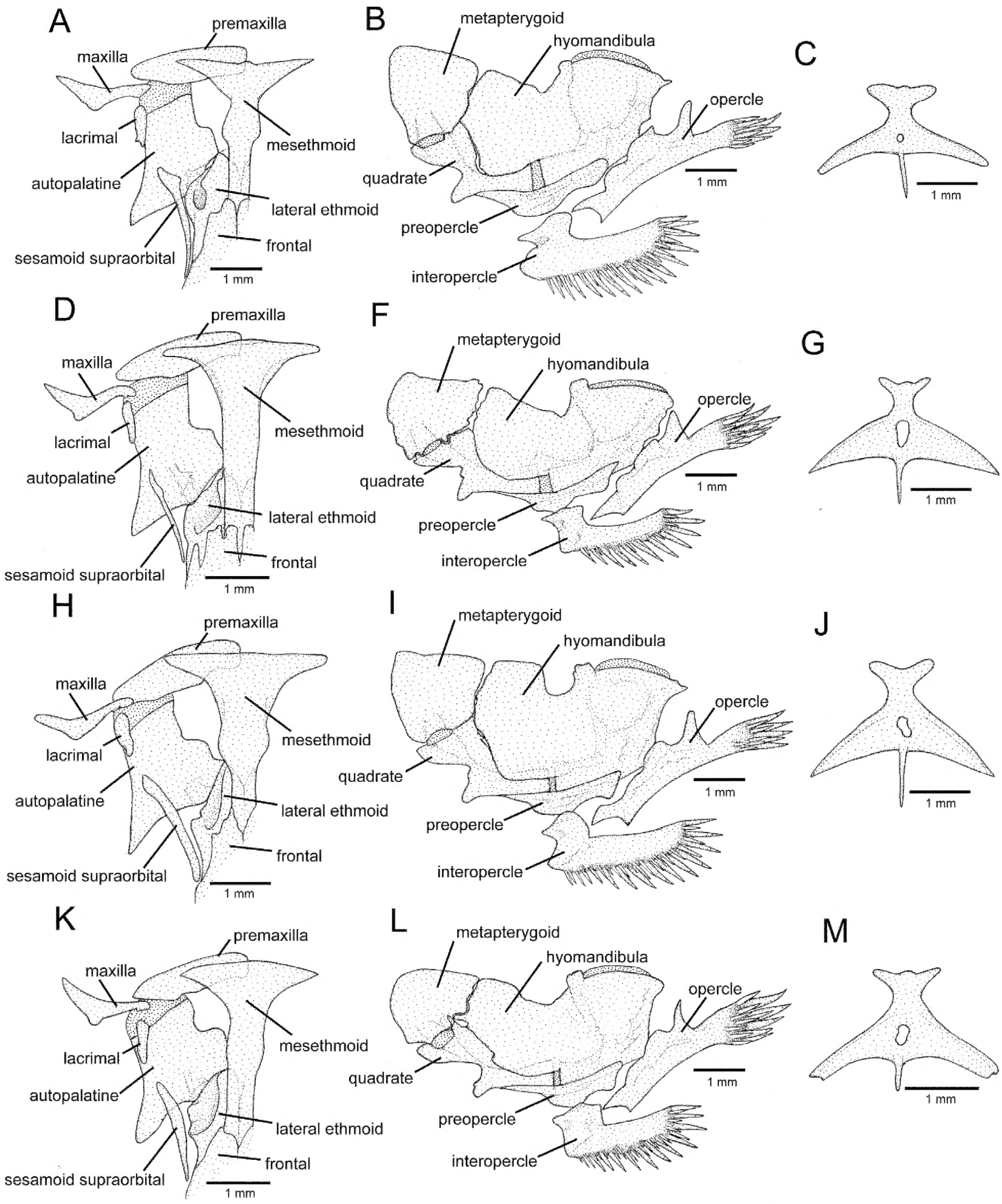

Figure 4. Osteological structures of: **A–C.** *Cambeva galacttica* Costa, Feltrin & Katz, sp. nov.; **D–F.** *Cambeva atrobrunnea* Costa, Feltrin & Katz, sp. nov.; **G–I.** *Cambeva luteoreticulata* Costa, Feltrin & Katz, sp. nov., and **J–L.** *Cambeva rotundipinna* Costa, Feltrin & Katz, sp. nov. **A, D, G, J.** Mesethmoidal region and adjacent structures, left and middle portions, dorsal view; **B, E, H, K.** Left jaw suspensorium and opercular series, lateral view. **C, F, I, L.** Parurohyal, ventral view. Abbreviation of structure indicated by arrow: aes, anteromedial expansion of sesamoid supraorbital. Larger stippling represents cartilaginous areas.

CYTB 528 (A→G), CYTB 585 (T→C)**, CYTB 711 (C→T)*, CYTB 715 (G→A)*, CYTB 735 (C→T)*, CYTB 771 (C→T)*, CYTB 822 (A→G), CYTB 849 (T→C), CYTB 891 (T→C)*, CYTB 900 (T→C)*, CYTB 909 (A→G), CYTB 994 (A→C), CYTB 1032 (C→T)**. COX1 p-distances among congeners of the *Cambeva* beta-clade ranging from 2.9 (*Cambeva atrobrunnea* Costa, Feltrin & Katz, sp. nov. and *Cambeva ventropapillata* Costa, Feltrin & Katz, 2022) and 4.7.

Description. Morphometric data appear in Table 3.

Table 3. Morphometric data of *Cambeva galactica* Costa, Feltrin & Katz, sp. nov.

	Holotype	Paratypes (n = 6)
Standard length (SL)	76.9	40.1–108.0
Percentage of standard length		
Body depth	16.4	15.1–16.2
Caudal peduncle depth	11.8	10.5–12.7
Body width	11.6	9.8–12.6
Caudal peduncle width	4.5	3.4–5.5
Pre-dorsal length	65.3	62.6–65.8
Pre-pelvic length	60.0	58.5–62.4
Dorsal-fin base length	10.9	11.1–12.2
Anal-fin base length	9.3	8.4–10.0
Caudal-fin length	17.6	15.4–18.3
Pectoral-fin length	13.3	11.6–14.4
Pelvic-fin length	9.9	8.7–9.4
Head length	22.5	20.6–23.1
Percentage of head length		
Head depth	44.3	42.2–52.0
Head width	80.4	78.5–90.5
Snout length	42.1	35.1–43.6
Interorbital width	24.4	25.5–26.9
Preorbital length	11.9	9.7–11.7
Eye diameter	9.7	6.9–11.9

Head morphology. Barbels moderate in length. Nasal barbel reaching area just anterior to opercle, maxillary barbel reaching between interopercular patch of odontodes and pectoral-fin base, and rictal barbel reaching posterior portion of interopercular patch of odontodes. Jaw teeth pointed, irregularly arranged. Premaxillary teeth 41–43, dentary teeth 39–46. Opercular and interopercular odontodes pointed, about straight. Opercular odontodes 8 or 9; interopercular odontodes 29–32. Anterior infraorbital sensory canal present.

Fin morphology. Dorsal and anal fins subtriangular, margins slightly convex. Total dorsal-fin rays 11 or 12 (ii–iii + II–III + 6–7), total anal-fin rays 9 or 10 (ii–iii + II + 5). Anal-fin origin at vertical just posterior to middle dorsal-fin base, at base of 3rd or 4th branched dorsal-fin ray. Pectoral fin sub-triangular in dorsal view, margins slightly convex, first pectoral-fin ray slightly longer than second ray, weakly extending beyond fin membrane forming minute filament. Total pectoral-fin rays 6 (I + 5). Pelvic fin rounded, its tip reaching vertical through middle portion of dorsal-fin base. Total pelvic-fin rays 5 (I + 4). Caudal fin subtruncate, corners rounded. Total principal caudal-fin rays 13 (I + 11 + I), total dorsal procurrent rays 18 or 19 (xvii–xviii + I), total ventral procurrent rays 12 or 13 (xi–xii + I).

***Osteology* (Fig. 4A–C).** Mesethmoid narrow anteriorly, with lateral expansion in area just anterior to lateral ethmoid, anterior mesethmoid margin slightly concave, with minute anterior projection on its middle portion. Mesethmoid cornu extremity pointed. Lateral ethmoid with small lateral projection immediately posterior to articular facet for autopalatine. Anterodorsal portion of lateral ethmoid widened, projecting laterally. Lacrimal thin, elliptical. Sesamoid supraorbital gently curved, its longitudinal length about two times and half longer than lacrimal longitudinal length, its largest width about equal to lacrimal width. Medial margin of anterior portion of sesamoid supraorbital with distinctive projection, connected by thin ligamentous tissue to dorsal projection on articulatory shell of autopalatine for lateral ethmoid. Premaxilla long, laterally narrowing. Maxilla slender, with rudimentary posterior process, slightly curved, its length about four fifths of premaxilla. Autopalatine sub-trapezoidal in dorsal view, medial margin sinuous, lateral margin weakly concave. Autopalatine postero-lateral process triangular, short, its length about half autopalatine length.

Metapterygoid trapezoid, deeper than long, large, its surface about twice quadrate lateral surface. Quadrate with deep anterior constriction at dorsal process base. Hyomandibula long, anterior outgrowth horizontal length longer than largest horizontal metapterygoid length. Posterior margin of hyomandibula with small projection just above articular facet for opercle. Dorsal margin of hyomandibula outgrowth concave. Opercle elongate, longer than interopercle. Opercular odontode patch very slender, its depth about one third hyomandibula articular facet length. Dorsal process of opercle short, subtriangular, its extremity rounded. Opercular articular facet for hyomandibula with dorsal, rounded laminar projection. Articular facet for preopercle rounded, well-developed. Interopercle relatively long, interopercular odontode patch length longer than hyomandibula outgrowth length. Preopercle slender, with minute ventral projection.

Parurohyal thin, lateral process narrow, slightly curved posteriorly, with rounded extremity. Parurohyal head with prominent anterolateral paired process. Parurohyal middle foramen small, rounded. Parurohyal posterior process moderate in length, about three fourths of distance between anterior margin of parurohyal and anterior insertion of posterior process. Branchiostegal rays 8. Vertebrae 39 or 40. Ribs 14 or 15. Dorsal-fin origin at vertical through centrum of 21st or 22nd vertebra; anal-fin origin at vertical through centrum of 21st or 22nd vertebra. Two dorsal and single ventral hypural plate.

Colouration in alcohol. In adult specimens (Fig. 2), flank, dorsum, and head side pale brown; three longitudinal rows of interconnected yellowish white, diffuse, vermiculate marks: row on dorsum, with marks forming reticulate pattern along pre-dorsal midline; one row on dorsal portion of flank, comprising minute marks; and row on ventral portion of flank. Venter and ventral surface of head yellowish white. Barbels pale brown. Fins greyish hyaline. In juvenile specimens between about 25 and 50 mm SL (Fig. 3), flank and dorsum pale yellow, with broad dark brown stripe along flank longitudinal midline and dark brown reticulate pattern on dorsum, and dorsal and ventral portions of flank. In juvenile specimens smaller than 20 mm SL, flank and dorsum pale yellow, with narrow black stripe along flank longitudinal midline and longitudinal series of black blotches between dorsum and flank, and longitudinal series of small black dots on ventral portion of flank.

Distribution. *Cambeva galactica* is only known from its type locality in the upper Rio Preto drainage, which is a tributary of the Rio Negro, Rio Iguaçu drainage, Rio Paraná basin, at about 970 m asl (Fig. 5).

Etymology. The name *galactica* is derived from the Ancient Greek word galaktikós meaning milky, an allusion to the rows of yellowish white diffuse vermiculate marks present in the flank of the new species, reminiscent of the Milky Way.

Western RISE species

Cambeva atrobrunnea Costa, Feltrin & Katz, sp. nov.

https://zoobank.org/A2FF0368-0311-4739-9CB2-415343090897

Figs 4D–F, 6, 7, Table 4

Type material. ***Holotype.*** Brazil • 70.1 mm SL; Santa Catarina State: Timbó Grande Municipality: stream tributary of Rio Timbó, Rio Iguaçu drainage, Rio Paraná basin; 26°34'41"S, 50°40'28"W; about 970 m asl; 29 Jun. 2023; C.R.M. Feltrin, leg; UFRJ 14066.

Paratypes. Brazil • 7 ex., 26.6–70.1 mm SL; same data as holotype; UFRJ 13821. • 2 ex. (C&S), 27.4–44.2 mm SL; same data as holotype; UFRJ 14067. • 2 ex., 29.9–46.8 mm SL. same locality and collector as holotype; 31 Mar. 2023; UFRJ 13553. • 3 ex. (DNA), 27.4–44.2 mm SL; same locality and collector as holotype; 31 Mar. 2023; UFRJ 13554.

Diagnosis. *Cambeva atrobrunnea* is distinguished from all other congeners by having the two posterior-most dorsal and ventral procurrent caudal-fin rays segmented (vs. only the posterior-most ray segmented). *Cambeva atrobrunnea* is also distinguished from the two other species of western RISE, *Cambeva luteoreticulata* Costa, Feltrin & Katz, sp. nov. and *Cambeva rotundipinna* Costa, Feltrin & Katz, sp. nov., by having subtruncate caudal fin (vs. rounded), fewer interopercular odontodes (20–22 vs. 29–34), and specimens below about 40 mm SL having flank light grey with small black dots that are arranged in irregular rows, coalesced on the anterior portion of the longitudinal midline to form a stripe (Fig. 7A; vs. pale yellow with large, irregularly shaped dark brown to black blotches, sometimes forming longitudinal stripes in the area between dorsum and flank in *C. luteoreticulata* Costa, Feltrin & Katz, sp. nov., and light brownish yellow with small black dots irregularly arranged in *C. rotundipinna* Costa, Feltrin & Katz, sp. nov. (see descriptions below); from *C. luteoreticulata* Costa, Feltrin & Katz, sp. nov. by specimens above 40 mm SL having the nasal barbel reaching area just anterior to opercle (vs. reaching area anterior to orbit), fewer ventral procurrent caudal-fin rays (13 or 14 vs. 15 or 16), and jaw teeth irregularly arranged (vs. arranged in three rows); and from *C. rotundipinna* Costa, Feltrin & Katz, sp. nov. by having more procurrent caudal-fin rays (21 dorsal and 13 or 14 ventral, vs. 15–17 and 10 or 11, respectively), and more opercular odontodes (12 vs. eight or nine). *Cambeva atrobrunnea* is also distinguished from all the remaining congeners from the Rio Iguaçu drainage by the following combination of character states: seven pectoral-fin rays (vs. eight in *Cambeva castroi* (de Pinna, 1992), *Cambeva melanoptera* Costa,

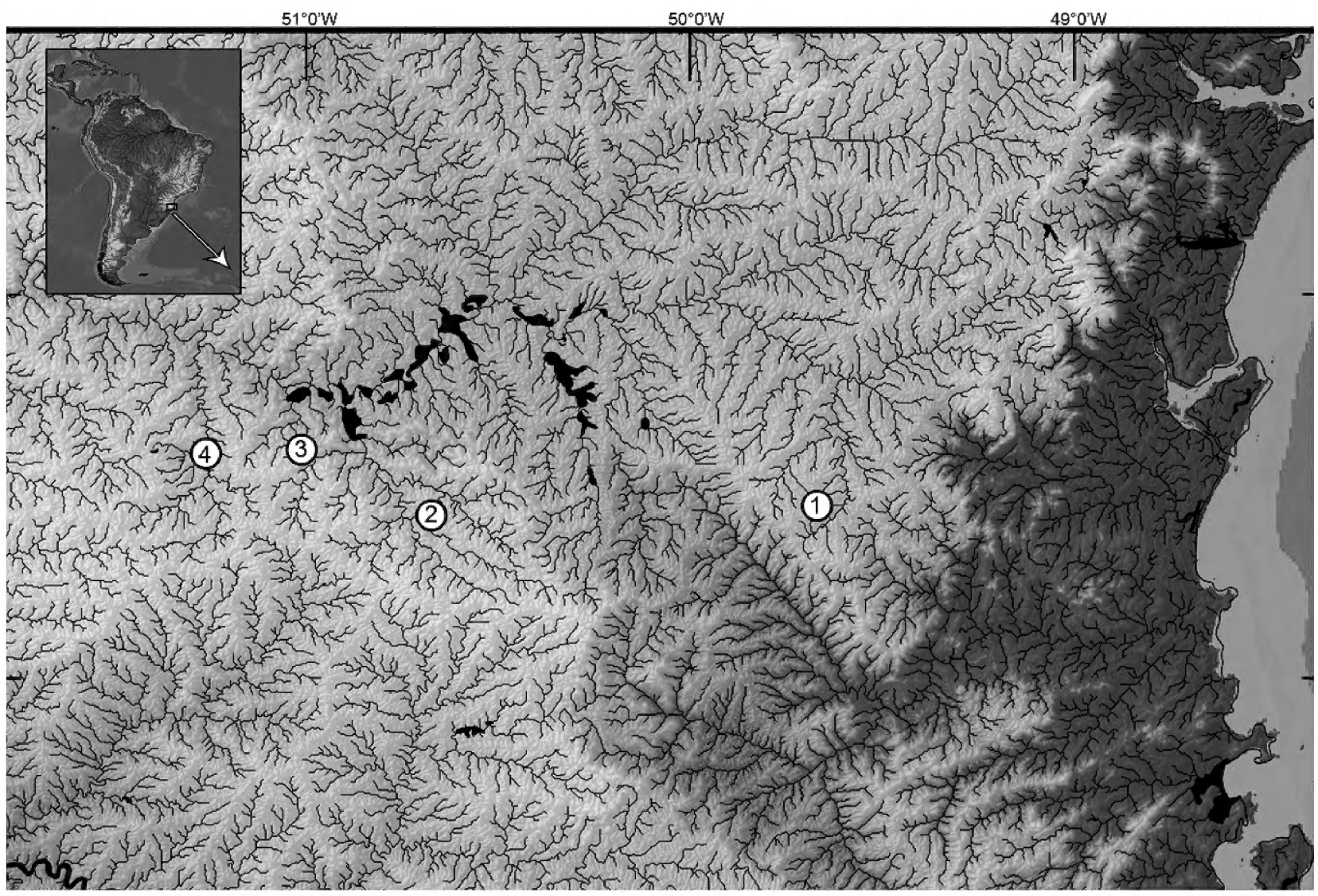

Figure 5. Geographical distribution of four new species of *Cambeva* from the Rio Iguaçu drainage, Serra do Espigão, southern Brazil: 1. *Cambeva galactica* Costa, Feltrin & Katz, sp. nov.; 2. *Cambeva atrobrunnea* Costa, Feltrin & Katz, sp. nov.; 3. *Cambeva luteoreticulata* Costa, Feltrin & Katz, sp. nov.; 4. *Cambeva rotundipinna* Costa, Feltrin & Katz, sp. nov.

Figure 6. *Cambeva atrobrunnea* Costa, Feltrin & Katz, sp. nov., holotype, UFRJ 14066, 70.1 mm SL. **A.** Lateral view; **B.** Dorsal view; **C.** Ventral view.

Abilhoa, Dalcin & Katz, 2022, *Cambeva crassicaudata* (Wosiacki & de Pinna, 2008), *Cambeva stawiarski* (Miranda Ribeiro, 1968), and six in *C. galactica*, *C. naipi*, and *C. taroba*); absence of the anterior infraorbital (vs. presence in *C. galactica*, *C. naipi*, *Cambeva papillifera* (Wosiacki & Garavello, 2004), *Cambeva plumbea* (Wosiacki & Garavello, 2004), and *C. taroba*); posterior margin of the caudal fin slightly convex (vs. about straight in *C. crassicaudata*, *C. davisi*, *C. galactica*, *C. melanoptera*, *C. papillifera*, *Cambeva piraquara* dos Reis, Wosiacki, Ferrer, Donin & da Graça, 2022, *C. plumbea*, *C. igobi* (Wosiacki & de Pinna, 2008); straight to slightly concave in *C. stawiarski*; bilobed in *C. crassicaudata*; and emarginate in *Cambeva cauim* dos Reis, Ferrer & Graça, 2021); absence of hypertrophied papillae on the ventral surface of the head (vs. presence in *C. papillifera*); absence of pectoral-fin filament (vs. presence a well-developed filament in *C. taroba* and a rudimentary filament in *C. davisi*, *C. galactica*, and *C. piraquara*); 12 opercular odontodes (vs. broad, with 17 or 18 in *Cambeva mboycy* (Wosiacki & Garavello, 2004); 15 or 16 in *C. davisi*; seven or eight in *C. taroba*); 20–22 interopercular odontodes (vs. 12 or 13 in *C. naipi*); 21 dorsal procurrent caudal-fin rays (vs. 15–17 in *C. castroi* and *C. melanoptera*; 18 or 19 in *C. naipi*; 25–29 in *C. crassicaudata*, *C. igobi*, *C. mboycy*, *C. stawiarski*, and *C. taroba*; 30 or 31 in *C. cauim*); 13 or 14 ventral procurrent caudal-fin rays (vs. 21 – 23 in *C. taroba*); dorsal-fin origin at a vertical through the centrum of the 21st or 22nd vertebra (vs. 19th or 20th in *C. crassicaudata*, *C. mboycy*, and *C. stawiarski*); jaw teeth pointed, irregularly arranged (vs. incisiform and arranged in rows in *C. davisi*); and 39 or 40 vertebrae (36 in *C. taroba*). Molecular diagnosis: combination of 17 nucleotide substitutions, five of them unique among taxa analysed*, and four unique for the *Cambeva* beta-clade **: COX1 216 (A→C)*, COX1 249 (T→C), COX1 252 (G→A), COX1 471 (G→A), COX1 534 (G→A), CYTB 108 (C→T), CYTB 186 (C→T)**, CYTB 237 (C→T)*, CYTB 360 (T→C)**, CYTB 378 (C→T)*, CYTB 442 (C→T)*, CYTB 765 (C→T), CYTB 909 (A→T)**, CYTB 942 (A→G), CYTB 960 (A→T)*, CYTB 994 (A→C). COX1 p-distances among congeners of the *Cambeva* beta-clade ranging from 1.2 (*Cambeva chrysornata* Costa, Feltrin & Katz, 2022 and *Cambeva rotundipinna* Costa, Feltrin & Katz, sp. nov.) and 3.9.

Description. Morphometric data appear in Table 4.

***Head morphology*.** Barbels moderate in length. Nasal barbel reaching between orbit and opercular patch of odontodes, maxillary barbel reaching posterior portion of interopercular patch of odontodes, and rictal barbel reaching middle of interopercular patch of odontodes. Jaw teeth variable in shape, smaller teeth slightly pointed, larger teeth sub-incisiform with slightly rounded tip, irregularly arranged. Premaxillary teeth 39–41, dentary

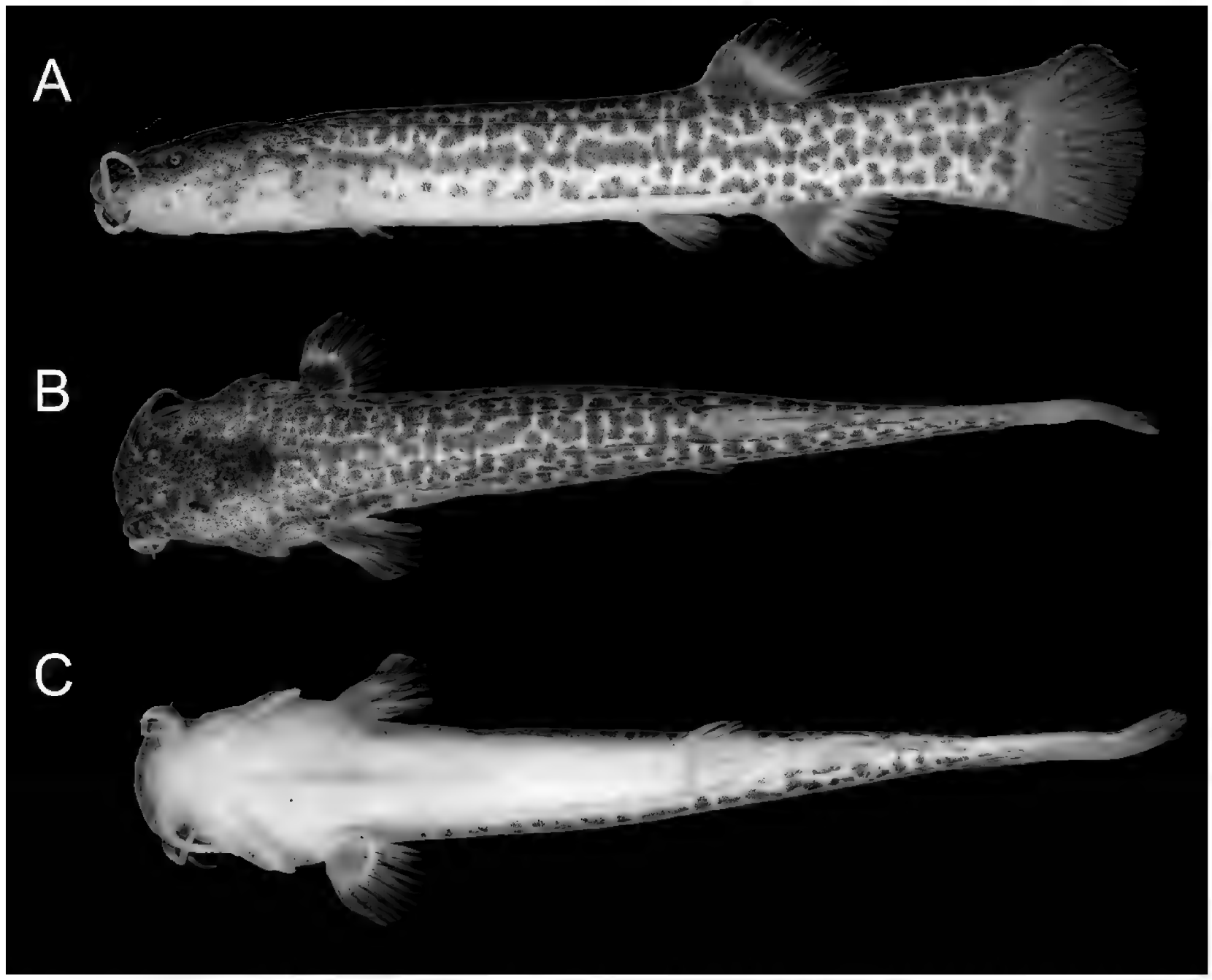

Figure 7. *Cambeva atrobrunnea* Costa, Feltrin & Katz, sp. nov., paratype, UFRJ 13821, 33.4 mm SL. **A.** Lateral view; **B.** Dorsal view; **C.** Ventral view.

Table 4. Morphometric data of *Cambeva atrobrunnea* Costa, Feltrin & Katz, sp. nov.

	Holotype	Paratypes (n = 5)
Standard length (SL)	70.1	46.8–78.5
Percentage of standard length		
Body depth	14.2	12.2–15.0
Caudal peduncle depth	13.7	11.2–13.1
Body width	12.1	10.3–12.8
Caudal peduncle width	4.3	3.0–5.0
Pre-dorsal length	67.7	63.5–67.2
Pre-pelvic length	62.7	57.9–60.3
Dorsal-fin base length	13.4	10.9–12.5
Anal-fin base length	10.0	9.0–12.7
Caudal-fin length	17.1	16.0–19.0
Pectoral-fin length	12.0	11.6–13.1
Pelvic-fin length	8.7	9.1–12.4
Head length	22.3	19.5–24.7
Percentage of head length		
Head depth	43.9	39.7–51.9
Head width	82.7	65.6–88.0
Snout length	39.9	36.1–46.6
Interorbital width	20.3	18.3–23.6
Preorbital length	12.2	10.6–15.4
Eye diameter	8.4	8.2–12.4

teeth 40. Opercular and interopercular odontodes pointed, about straight. Opercular odontodes 12; interopercular odontodes 20–22. Anterior infraorbital sensory canal absent.

Fin morphology. Dorsal and anal fins subtriangular, distal margin slightly convex. Total dorsal-fin rays 10 or 11 (ii + II–III + 6–7), total anal-fin rays 9 or 10 (ii + II + 5–6). Anal-fin origin at vertical just posterior to middle of dorsal-fin base, at base of 4th branched dorsal-fin ray. Pectoral fin sub-triangular in dorsal view, margins slightly convex, first pectoral-fin ray shorter than second ray, not forming terminal filament. Total pectoral-fin rays 7 (I + 6). Pelvic fin rounded, its tip reaching vertical through anterior portion of dorsal-fin base. Total pelvic-fin rays 5 (I + 4). Caudal fin subtruncate, posterior margin weakly convex. Total principal caudal-fin rays 13 (I + 11 + I), total dorsal procurrent rays 21 (xix + II), total ventral procurrent rays 13 or 14 (xi–xii + II).

***Osteology* (Fig. 4D–F).** Mesethmoid broader anteriorly, without lateral expansions in its main axis, anterior mesethmoid margin slightly convex. Mesethmoid cornu extremity rounded. Lateral ethmoid with small lateral projection immediately posterior to articular facet for autopalatine and small, twisted expansion on anterior margin. Lacrimal narrow, short and thin. Sesamoid supraorbital rod-shaped, narrower than lacrimal, its longitudinal length about two times and half longer than lacrimal longitudinal length, without lateral expansions. Premaxilla long, laterally narrowing, slightly curved. Maxilla slender, with rudimentary posterior process, slightly curved, its length about three fourths of premaxilla. Autopalatine

sub-trapezoidal in dorsal view, medial margin sinuous, lateral margin weakly concave. Autopalatine postero-lateral process triangular, short, its length about half autopalatine length excluding anterior cartilage. Autopalatine articulation for lateral ethmoid with laminar shovel-shaped expansion.

Metapterygoid sub-rectangular, longer than deep, relatively large, its surface greater than quadrate lateral surface. Areas anterior and posterior to cartilaginous articulation between metapterygoid and quadrate with small laminar overlapped expansions forming additional points of articulation. Quadrate with deep anterior constriction at dorsal process base. Hyomandibula long, anterior outgrowth horizontal length slightly longer than largest horizontal metapterygoid length; dorsal margin of hyomandibula outgrowth concave. Opercle elongate, longer than interopercle. Opercular odontode patch slender, its depth about half hyomandibula articular facet length. Dorsal process of opercle short, subtriangular, its extremity rounded. Opercular articular facet for hyomandibula with dorsal, trapezoidal laminar projection, articular facet for preopercle small, rounded. Interopercle moderate in length, interopercular odontode patch length about equal hyomandibula outgrowth length. Preopercle slender, with minute ventral projection.

Parurohyal robust, lateral process subtriangular, slightly curved posteriorly, with pointed tip. Parurohyal head with prominent anterolateral paired process. Parurohyal middle foramen relatively large, oval. Parurohyal posterior process moderate in length, about half of distance between anterior margin of parurohyal and anterior insertion of posterior process. Branchiostegal rays 9. Vertebrae 39 or 40. Ribs 14 or 15. Dorsal-fin origin at vertical through centrum of 21st or 22nd vertebra; anal-fin origin at vertical through centrum of 25th or 26th vertebra. Two or one dorsal and single ventral hypural plate.

Colouration in alcohol. In adult specimens (Fig. 6), flank, dorsum, and head side light brownish yellow, with great concentration of small dark brown to black dots. Venter and ventral surface of head brownish white, with minute dark brown dots in area just anterior to pelvic fin. Nasal and maxillary barbels brown, rictal barbel brownish white. Fins hyaline, with minute dark brown dots on basal region of dorsal, anal and pectoral fins, and on whole caudal fin. In juvenile specimens below about 50 mm SL (Fig. 7), flank, dorsum and head side light grey, with small black dots arranged in irregular longitudinal rows, coalesced on anterior portion of longitudinal midline of flank to form black stripe.

Distribution. *Cambeva atrobrunnea* is known from a single locality in a stream tributary of the Rio Timbó, Rio Iguaçu drainage, Rio Paraná basin, at about 970 m asl (Fig. 5).

Etymology. From the Latin ater (dull black, dark) and brunneus (brown), referring to the predominant colour of the flank in adult specimens of the new species.

Cambeva luteoreticulata Costa, Feltrin & Katz, sp. nov.

https://zoobank.org/E144F2B3-9DEE-4A23-930B-B5B336070D65

Figs 4G–I, 8, 9, Table 5

Type material. ***Holotype.*** Brazil • 81.6 mm SL; Santa Catarina State: Matos Costa Municipality: village of Colônia Cerne: stream tributary of Rio Liso, itself a tributary of Rio Pintado, Rio Iguaçu drainage, Rio Paraná basin; 26°24'25"S, 51°00'45"W; about 1,015 m asl; 1 Apr. 2023; C.R.M. Feltrin and L. Sebben, leg.; UFRJ 14068.

Paratypes. Brazil • 7 ex. 25.2–70.8 mm SL; same data as holotype; UFRJ 13562. • 3 ex. (DNA), 22.7–42.6 mm SL; same data as holotype; UFRJ 13563. • 15 ex., 27.6–77.2 mm SL; same locality and collectors as holotype; 1 Jul. 2023; UFRJ 13828. • 4 ex. 33.7–75.9 mm SL; same locality and collectors as holotype; 1 Jul. 2023; CICCAA 08268. • 4 ex. (C&S), 38.2–65.9 mm SL; same locality and collectors as holotype; 1 Jul. 2023; UFRJ 14069.

Diagnosis. *Cambeva luteoreticulata* differs from all other congeners by its unique rounded, stapula-shaped caudal fin in specimens above about 40 mm SL (Fig. 8A). *Cambeva luteoreticulata* is also distinguished from all other congeners of the *Cambeva* beta-clade, except *Cambeva chrysornata* Costa, Feltrin, Mattos, Dalcin, Abilhoa & Katz, 2023 and *C. papillifera*, by having short barbels, with the nasal barbel not reaching the orbit in specimens above 60 mm SL and maxillary and rictal barbels not reaching the interopercular patch of odontodes. *Cambeva luteoreticulata* also differs from *C. chrysornata* and *C. papillifera* by the absence of the anterior segment of the infraorbital series (vs. presence), from *C. chrysornata* by having more procurrent caudal-fin rays (21 or 22 dorsal and 15 or 16 ventral, vs. 16 or 17 and 11 or 12, respectively) and fewer opercular odontodes (10–12 vs. 18), and from *C. papillifera* by the absence of hypertrophied papillae on the head surface (vs. presence) and narrow nasal barbel (vs. broad laminar, ribbon-shaped). *Cambeva luteoreticulata* is also distinguished from all other congeners by a unique pattern of ontogenetic colouration change consisting of flank pale yellow with irregularly shaped and arranged, dark brown to black blotches in specimens below about 40 mm SL (Fig. 9A), becoming dark brown, with small, irregularly shaped pale yellow marks forming reticulate pattern in larger specimens (Fig. 8A). *Cambeva luteoreticulata* also differs from all the remaining congeners from the Rio Iguaçu drainage by the following combination of character states: seven pectoral-fin rays (vs. eight in *C. castroi*, *C. melanoptera*, *C. crassicaudata*, *C. stawiarski*; and six in *C. galactica*, *C. naipi*, and *C. taroba*); absence of the anterior infraorbital (vs. presence in *C. galactica*, *C. naipi*, *C. plumbea*, and *C. taroba*); posterior margin of the caudal fin convex (vs. about straight in *C. crassicaudata*, *C. davisi*, *C. galactica*, *C. melanoptera*, *C. papillifera*, *C. piraquara*, *C. plumbea*, *C. igobi*; straight to slightly concave in *C. stawiarski*; bilobed in *C. crassicaudata*;

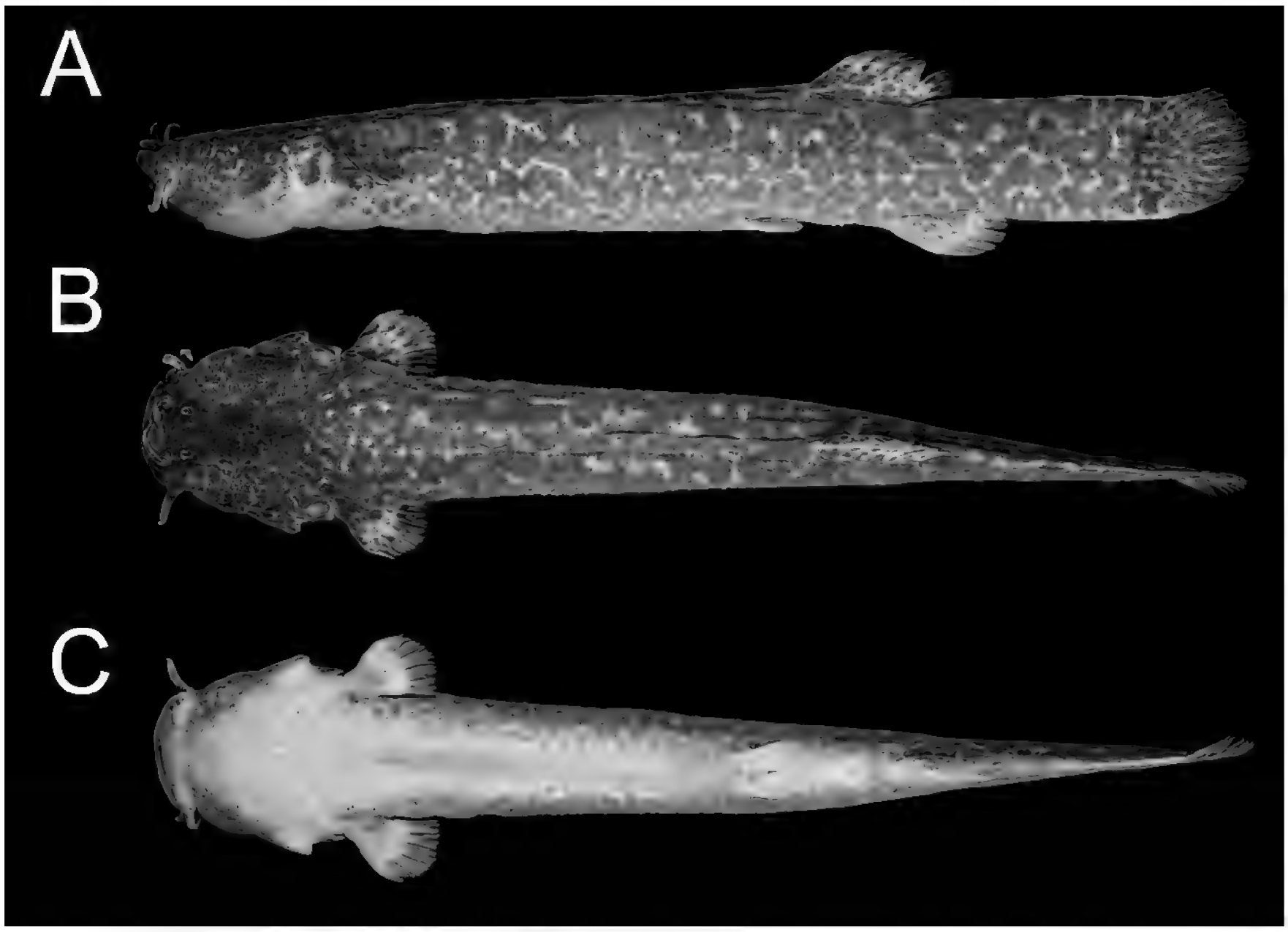

Figure 8. *Cambeva luteoreticulata* Costa, Feltrin & Katz, sp. nov., holotype, UFRJ 14068, 81.6 mm SL. **A.** Lateral view; **B.** Dorsal view; **C.** Ventral view.

and emarginate in *Cambeva cauim*); absence of pectoral-fin filament (vs. presence a well-developed filament in *C. taroba* and a rudimentary filament in *C. davisi* and *C. piraquara*); nine or 10 opercular odontodes (vs. broad, with 17 or 18 in *C. mboycy*; 15 or 16 in *C. davisi*; seven or eight in *C. taroba*); 29–32 interopercular odontodes (vs. 12 or 13 in *C. naipi*; 17–21 in *C. mboycy* and *C. taroba*); 25 dorsal procurrent caudal-fin rays (vs. 15–17 in *C. castroi* and *C. melanoptera*; 18 or 19 in *C. naipi*;; 30 or 31 in *C. cauim*); 15 or 16 ventral procurrent caudal-fin rays (vs. 21–23 in *C. taroba*); dorsal-fin origin at a vertical through the centrum of the 21st or 22nd vertebra (vs. 19th or 20th in *C. crassicaudata*, *C. mboycy*, and *C. stawiarski*); larger jaw teeth incisiform, teeth arranged in rows (vs. pointed to slight rounded, irregularly arranged in all species, except *C. davisi*); and 38–40 vertebrae (36 in *C. taroba*). Molecular diagnosis: 17 nucleotide substitutions, five of them unique among taxa analysed* and one unique for the *Cambeva* beta-clade **: COX1 252 (A→G), COX1 564 (A→C)*, COX1 648 (C→T)*, COX1 678 (A→G), CYTB 123 (C→T), CYTB 206 (G→C)*, CYTB 294 (C→T)*, CYTB 474 (G→A), CYTB 495 (G→A), CYTB 636 (C→T)*, CYTB 675 (T→C), CYTB 696 (A→G), CYTB 696 (A→G), CYTB 879 (A→G)**, CYTB 988 (G→A), CYTB 996 (A→G), CYTB 1038 (C→T). COX1 p-distances among congeners of the *Cambeva* beta-clade ranging from 1.5 (*Cambeva atrobrunnea* Costa, Feltrin & Katz, sp. nov. and *Cambeva rotundipinna* Costa, Feltrin & Katz, sp. nov.) and 4.3.

Description. Morphometric data appear in Table 5.

Table 5. Morphometric data of *Cambeva luteoreticulata* Costa, Feltrin & Katz, sp. nov.

	Holotype	**Paratypes (n = 10)**
Standard length (SL)	81.6	44.4–77.2
Percentage of standard length		
Body depth	13.6	13.3–16.0
Caudal peduncle depth	12.7	11.8–13.8
Body width	10.1	10.3–12.8
Caudal peduncle width	4.1	3.3–5.4
Pre-dorsal length	67.9	61.0–67.8
Pre-pelvic length	61.3	59.3–65.2
Dorsal-fin base length	11.0	10.6–12.3
Anal-fin base length	8.6	7.8–9.5
Caudal-fin length	13.1	11.5–16.1
Pectoral-fin length	9.6	8.1–12.7
Pelvic-fin length	7.2	5.8–8.9
Head length	21.6	21.4–23.8
Percentage of head length		
Head depth	45.0	42.6–51.7
Head width	80.3	78.1–84.1
Snout length	40.3	37.9–42.4
Interorbital width	21.2	18.7–24.6
Preorbital length	13.7	9.8–14.1
Eye diameter	8.2	8.6–12.2

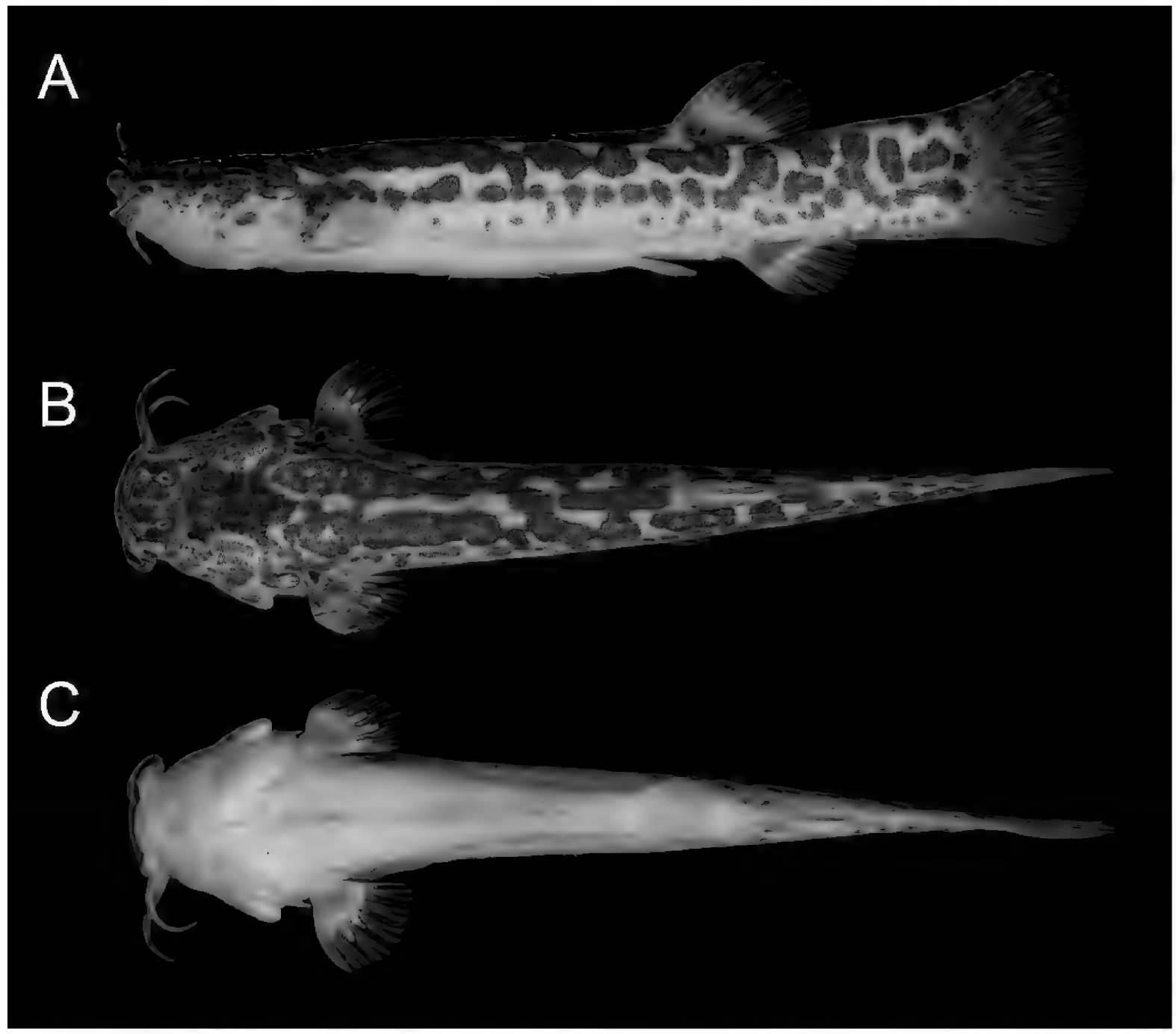

Figure 9. *Cambeva luteoreticulata* Costa, Feltrin & Katz, sp. nov., paratype, UFRJ 13562, 33.1 mm SL. **A.** Lateral view; **B.** Dorsal view; **C.** Ventral view.

***Head morphology*.** Barbels short. Nasal barbel reaching area anterior to orbit in specimens above 60 mm SL, between orbit and area just posterior to it in smaller specimens, and maxillary and rictal barbels reaching area just anterior to interopercular patch of odontodes. Jaw teeth variable in shape, smaller teeth slightly pointed, larger teeth incisiform with slightly rounded tip, arranged in three series. Premaxillary outer row with 14 or 15 teeth, middle row with 16 or 17 teeth, and inner row with 18 teeth; total premaxillary teeth 49. Dentary outer row with 10 or 11 teeth, middle row with 14 or 15 teeth, and inner row with 17–20 teeth; total dentary teeth 42–45. Opercular and interopercular odontodes pointed, about straight. Opercular odontodes 10–12; interopercular odontodes 29–33.

***Fin morphology*.** Dorsal and anal fins subtriangular, distal margin slightly convex. Total dorsal-fin rays 11 (ii + II + 7), total anal-fin rays 9 (ii + II + 5). Anal-fin origin at vertical through posterior portion of dorsal-fin base, at base of 5th branched dorsal-fin ray. Pectoral fin rounded in dorsal view, first pectoral-fin ray shorter than second ray, not forming terminal filament. Total pectoral-fin rays 7 (I + 6). Pelvic fin rounded, its tip reaching vertical through dorsal-fin origin. Total pelvic-fin rays 5 (I + 4). Caudal fin short, rounded, forming spatula-shaped tail in specimens above about 40 mm SL. Total principal caudal-fin rays 13 (I + 11 + I), total dorsal procurrent rays 21 or 22 (xx-xxi + I), total ventral procurrent rays 15 or 16 (xiv–xv + I).

***Osteology* (Fig. 4G–I).** Mesethmoid distinctively broader anteriorly, with lateral expansion in area just anterior to lateral ethmoid, anterior mesethmoid margin about straight to slightly convex. Mesethmoid cornu extremity rounded. Lateral ethmoid with small lateral projection immediately posterior to articular facet for autopalatine. Lacrimal thin, elliptical. Sesamoid supraorbital about two times and half longer than lacrimal, without lateral expansions, its width about equal to lacrimal width. Premaxilla long, laterally narrowing, slightly curved. Maxilla slender, without posterior process, slightly curved, its length about four fifths of premaxilla. Autopalatine sub-trapezoidal in dorsal view, medial margin sinuous, lateral margin weakly concave. Autopalatine postero-lateral process triangular, short, its length about half autopalatine length.

Metapterygoid sub-rectangular, deeper than long, relatively large, its surface greater than quadrate lateral surface. Quadrate with deep anterior constriction at dorsal process base. Hyomandibula long, anterior outgrowth horizontal length slightly longer than largest horizontal metapterygoid length; dorsal margin of hyomandibula outgrowth straight anteriorly, with pronounced U-shaped concavity posteriorly. Opercle elongate, longer than interopercle. Opercular odontode patch slender, its depth about half hyomandibula articular facet length. Dorsal process of opercle short, subtriangular, its extremity rounded. Opercular articular facet for hyomandibula with

dorsal, broad, rounded laminar projection, articular facet for preopercle rudimentary. Interopercle moderate in length, interopercular odontode patch length about equal hyomandibula outgrowth length. Preopercle slender, with minute ventral projection.

Parurohyal robust, lateral process subtriangular, slightly curved posteriorly, with pointed tip. Parurohyal head with prominent anterolateral paired process. Parurohyal middle foramen relatively large, oval. Parurohyal posterior process moderate in length, about three fifths of distance between anterior margin of parurohyal and anterior insertion of posterior process. Branchiostegal rays 9 or 10. Vertebrae 38–40. Ribs 14–16. Dorsal-fin origin at vertical through centrum of 21st or 22nd vertebra; anal-fin origin at vertical through centrum of 25th or 26th vertebra. Two dorsal and single ventral hypural plate.

Colouration in alcohol. In adult specimens (Fig. 8A), flank, dorsum and head side dark brown, with small, irregularly shaped, irregularly arranged, pale yellow marks forming reticulate pattern. Nasal and maxillary barbels brown, rictal barbel grey. Venter and ventral surface of head yellowish white. Fins pale grey with black spots on basal region, dark brown dots in middle region. In juvenile specimens below about 40 mm SL (Fig. 9A), flank, dorsum and head side pale yellow with large dark brown to black blotches, more concentrated and sometimes forming longitudinal stripes in area between dorsum and flank.

Distribution. *Cambeva luteoreticulata* is known from a single locality in a stream tributary of the Rio Liso, Rio Iguaçu drainage, Rio Paraná basin, at about 1,015 m asl (Fig. 5).

Etymology. From the Latin luteus (saffron yellow) and reticulata (reticulated), in reference to the flank colour pattern of adult specimens.

Cambeva rotundipinna Costa, Feltrin & Katz, sp. nov.

https://zoobank.org/1CD4DCB4-9F79-489D-B33E-420B2B935A57

Figs 4J–L, 10, 11, Table 6

Type material. ***Holotype.*** Brazil • 78.0 mm SL; Brazil: Santa Catarina State: Matos Costa Municipality: Paca road: Rio da Paca, tributary of Rio Jangada, Rio Iguaçu drainage, Rio Paraná basin; 26°25'02"S, 51°15'42"W; about 1000 m asl; 1 Apr. 2023; C.R.M. Feltrin and L. Sebben, leg.; UFRJ 14070.

Paratypes. All from Santa Catarina State: Matos Costa Municipality: Paca road: Rio da Paca, tributary of Rio Jangada, Rio Iguaçu drainage, Rio Paraná basin. Brazil • 2 ex., 44.4–76.3 mm SL; same data as holotype; UFRJ 13820. • 3 ex. (C&S), 30.3–55.2 mm SL; collected with holotype; UFRJ 14071. • 1 ex., 30.8 mm SL; collected with holotype; UFRJ 13559. • 1 ex. (DNA), 27.8 mm SL; 26°25'06"S, 51°16'30"W; about 1000 m asl; 30 Jun. 2023; C.R.M. Feltrin, leg.; UFRJ 13560.

Diagnosis. *Cambeva rotundipinna* differs from all other congeners of the *Cambeva* beta-clade, except *C. luteoreticulata*, by having a relatively short and rounded caudal fin in specimens above about 60 mm SL (Fig. 10A; vs. subtruncate, truncate, emarginate or forked). *Cambeva rotundipinna* differs from *C. luteoreticulata* by having fewer procurrent caudal-fin rays (15–17 dorsal and 10 or 11 ventral, vs. 21 or 22 and 15 or 16, respectively), jaw teeth irregularly arranged (vs. arranged in three rows), more opercular odontodes (14–17 vs. nine or ten), longer nasal barbel in specimens above 60 mm SL, reaching area between orbit and opercular patch of odontodes (vs. reaching area anterior to orbit), and a colour pattern of juveniles, in which the flank is light brownish yellow with small black dots irregularly arranged (vs. pale yellow with large, irregularly shaped dark brown to black blotches, more concentrated on its dorsal portion). *Cambeva rotundipinna* also differs from *C. atrobrunnea*, another species from western RISE, by having more odontodes (14–17 opercular and 30–34 interopercular, vs. 12 and 20–22, respectively) and a different juvenile colour pattern, comprising black dots irregularly arranged on the flank (Fig. 11A; vs. black dots arranged in irregular longitudinal rows, coalesced to form stripe on the anterior flank midline, Fig. 7A). *Cambeva rotundipinna* also differs from both *C. atrobrunnea* and *C. luteoreticulata* by having a broader autopalatine, with its largest width about equal to its length (Fig. 4J, vs. narrower, Fig. 4D, G) and a shorter posterior process of the parurohyal, its length about one third of the distance between the anterior margin of the parurohyal and the anterior insertion of the posterior process (Fig. 4L, vs. longer, Fig. 4F, I). *Cambeva rotundipinna* is also distinguished from all other species of *Cambeva* endemic to the Rio Iguaçu drainage by the following combination of character states: seven pectoral-fin rays (vs. eight in *C. castroi*, *C. melanoptera*, *C. crassicaudata*, *C. stawiarski*; and six in *C. galactica*, *C. naipi*, and *C. taroba*); absence of the anterior infraorbital (vs. presence in *C. galactica*, *C. naipi*, *C. papillifera*, *C. plumbea*, and *C. taroba*); posterior margin of the caudal fin convex (vs. about straight in *C. crassicaudata*, *C. davisi*, *C. galactica*, *C. melanoptera*, *C. papillifera*, *C. piraquara*, *C. plumbea*, *C. igobi*; straight to slightly concave in *C. stawiarski*; bilobed in *C. crassicaudata*; and emarginate in *C. cauim*); absence of hypertrophied papillae on the ventral surface of the head (vs. presence in *C. papillifera*); absence of pectoral-fin filament (vs. presence a well-developed filament in *C. taroba* and a rudimentary filament in *C. davisi* and *C. piraquara*); nine or 10 opercular odontodes (vs. broad, with 17 or 18 in *C. mboycy*; 15 or 16 in *C. davisi*; seven or eight in *C. taroba*); 30–34 interopercular odontodes (vs. 12 or 13 in *C. naipi*; 17–21 in *C. mboycy* and *C. taroba*); 15–17 dorsal procurrent caudal-fin rays (vs. 25–29 in *C. crassicaudata*, *C. igobi*, *C. mboycy*, *C. stawiarski*, and *C. taroba*; 30 or 31 in *C. cauim*); 10 or 11 ventral procurrent caudal-fin rays (vs. 15 or 16 in *C. naipi*, 21–23 in *C. taroba*); dorsal-fin origin at a vertical through the centrum of the 21st or 22nd vertebra (vs. 19th or 20th in *C. crassicaudata*, *C. mboycy*, and *C. stawiarski*); jaw teeth pointed, irregularly arranged (vs. incisiform and arranged in rows in *C. davisi*); and 39 vertebrae (36 in *C. taroba*). Molecular diagnosis: 10 nucleotide substitutions, two of

Figure 10. *Cambeva rotundipinna* Costa, Feltrin & Katz, sp. nov., holotype, UFRJ 14070, 78.0 mm SL. **A.** Lateral view; **B.** Dorsal view; **C.** Ventral view.

them unique among taxa analysed *: COX1 105 (G→A), COX1 252 (G→A), COX1 360 (G→A), COX1 462 (T→G)*, COX1 534 (G→A), CYTB 69 (A→G)*, CYTB 195 (T→C), CYTB 219 (T→C), CYTB 483 (A→G), CYTB 637 (G→A). COX1 p-distances among congeners of the *Cambeva* beta-clade ranging from 1.2 (*Cambeva atrobrunnea* Costa, Feltrin & Katz, sp. nov., *Cambeva cubataonis* (Bizerril, 1994), and *Cambeva ventropapillata* Costa, Feltrin & Katz, 2022) and 4.7.

Description. Morphometric data appear in Table 6.

Head morphology. Barbels moderate in length. Nasal barbel reaching area just posterior to orbit, maxillary and rictal barbels reaching middle of interopercular patch of odontodes. Jaw teeth with pointed to rounded extremities, irregularly arranged. Premaxillary teeth 37 or 38, dentary teeth 32–35 Opercular and interopercular odontodes pointed, about straight. Opercular odontodes 14–17, interopercular odontodes 30–34.

Fin morphology. Fins rounded. Total dorsal-fin rays 11 (ii + II + 7), total anal-fin rays 9 (ii + II + 5). Anal-fin origin at vertical through posterior portion of dorsal-fin base, at base of 6th branched dorsal-fin ray in specimens above about 50 mm SL, at vertical through posterior middle of dorsal-fin base, at base of 4th branched dorsal-fin ray in smaller specimens. Pectoral fin rounded in dorsal view, first pectoral-fin ray about equal in length to second ray, not forming terminal filament. Total pectoral-fin rays 7 (I + 6). Pelvic fin rounded, its tip reaching vertical through middle of dorsal-fin base. Total pelvic-fin rays 5 (I + 4). Caudal fin subtruncate, corners rounded. Total principal caudal-fin rays 13 (I + 11 + I), total dorsal procurrent rays 15–17 (xiv–xvi + I), total ventral procurrent rays 10 or 11 (ix–x + I).

Table 6. Morphometric data of *Cambeva rotundipinna* Costa, Feltrin & Katz, sp. nov.

	Holotype	**Paratypes (n = 3)**
Standard length (SL)	78.0	44.4–76.3
Percentage of standard length		
Body depth	15.1	14.5–15.6
Caudal peduncle depth	12.1	11.9–13.0
Body width	12.0	12.2–13.3
Caudal peduncle width	4.1	3.7–4.9
Pre-dorsal length	64.6	65.3–69.7
Pre-pelvic length	57.2	59.9–60.9
Dorsal-fin base length	11.5	11.4–12.2
Anal-fin base length	8.2	8.2–9.1
Caudal-fin length	14.0	14.8–16.6
Pectoral-fin length	9.4	9.6–12.6
Pelvic-fin length	8.2	8.4–9.4
Head length	19.9	21.6–25.9
Percentage of head length		
Head depth	50.7	40.7–52.7
Head width	85.3	68.6–80.1
Snout length	39.6	35.6–41.6
Interorbital width	22.2	18.7–23.7
Preorbital length	13.8	9.5–13.3
Eye diameter	8.3	7.9–10.2

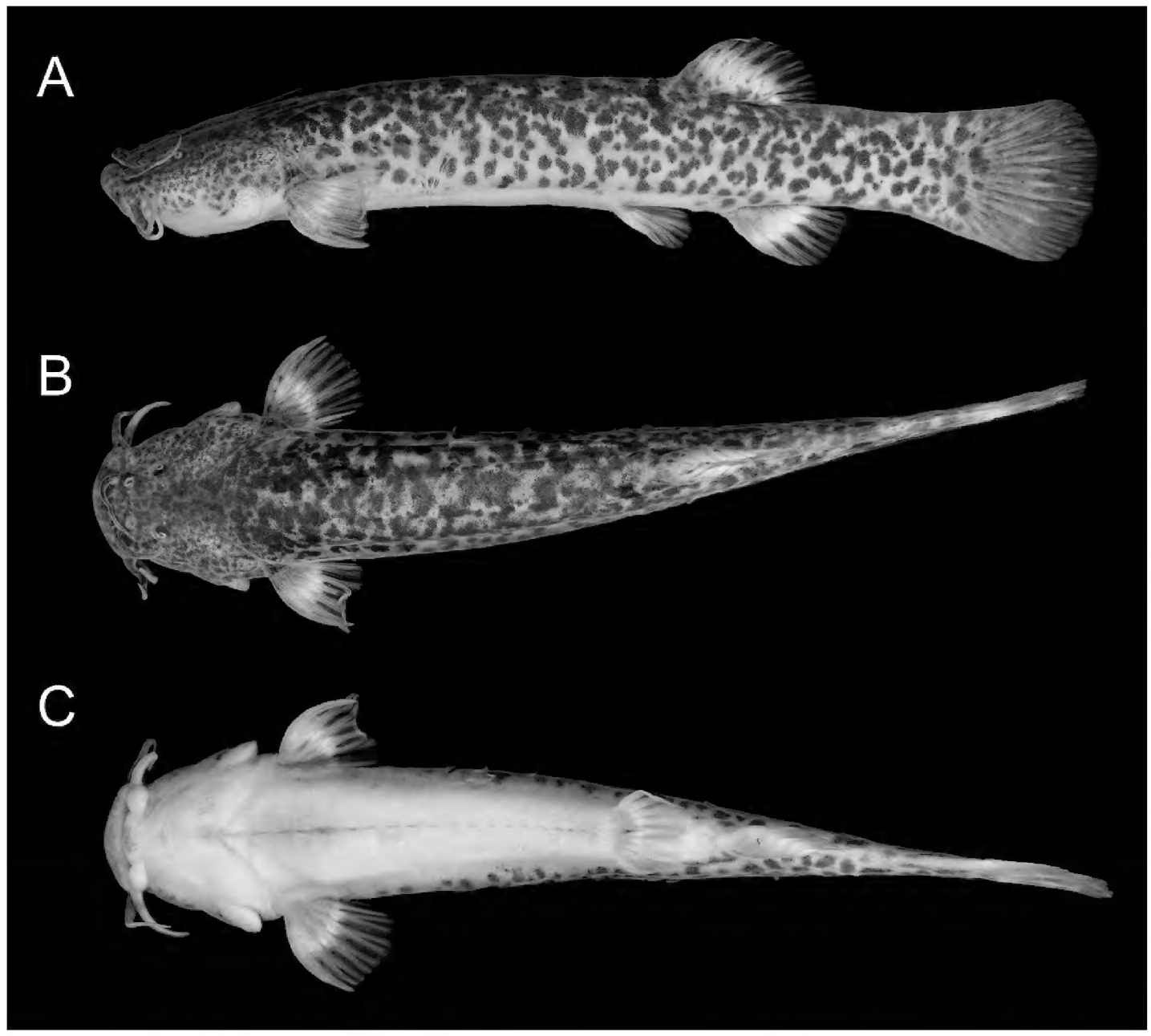

Figure 11. *Cambeva rotundipinna* Costa, Feltrin & Katz, sp. nov., paratype, UFRJ 13820, 44.0 mm SL. **A.** Lateral view; **B.** Dorsal view; **C.** Ventral view.

***Osteology* (Fig. 4J–L).** Mesethmoid broad anteriorly, with small lateral expansion in area just anterior to lateral ethmoid. Anterior mesethmoid margin convex, mesethmoid cornu broad, subtriangular, slightly curved posteriorly, abruptly narrowing at its extremity. Lateral ethmoid with small lateral projection immediately posterior to articular facet for autopalatine. Lacrimal thin, elliptical. Sesamoid supraorbital length about two times longer than lacrimal, without lateral expansions, its width about equal to lacrimal width. Premaxilla long, laterally narrowing, slightly curved. Maxilla slender, slightly curved, its length about four fifths of premaxilla, posterior process rudimentary. Autopalatine sub-trapezoidal in dorsal view, broad, its largest width about equal to its length, medial margin deeply sinuous with pronounced expansion on posterior margin, lateral margin weakly concave. Autopalatine postero-lateral process triangular, short, its length about half autopalatine length.

Metapterygoid sub-trapezoidal, longer than deep, relatively large, its surface greater than quadrate lateral surface. Area anterior to articulation between metapterygoid and quadrate with small laminar overlapped expansions of both bones. Quadrate with deep anterior constriction at dorsal process base. Hyomandibula long, anterior outgrowth horizontal length slightly longer than largest horizontal metapterygoid length. Dorsal margin of hyomandibula outgrowth concave. Opercle elongate, longer than interopercle. Opercular odontode patch moderately slender, its depth about two thirds of hyomandibula articular facet length. Dorsal process of opercle short, subtriangular, its extremity pointed. Opercular articular facet for hyomandibula with dorsal, small, rounded laminar projection, articular facet for preopercle rudimentary. Interopercle moderate in length, interopercular odontode patch length about equal hyomandibula outgrowth length. Preopercle slender, with minute ventral projection.

Parurohyal robust, lateral process sub-rectangular, slightly curved posteriorly, with truncate extremity. Parurohyal head with prominent anterolateral paired process. Parurohyal middle foramen relatively large, oval. Parurohyal posterior process short, about one third of distance between anterior margin of parurohyal and anterior insertion of posterior process. Branchiostegal rays 8 or 9. Vertebrae 39. Ribs 14 or 15. Dorsal-fin origin at vertical through centrum of 21st or 22nd vertebra; anal-fin origin at vertical through centrum of 25th or 26th vertebra. Two dorsal and single ventral hypural plate.

Colouration in alcohol. In adult specimens, above about 50 mm SL (Fig. 10), flank, dorsum and head side light brownish yellow, with great concentration of small dark brown to black dots. Venter and ventral surface of head pale yellow, with minute dark brown dots in area just anterior to pelvic fin and on branchiostegal region. Nasal and maxillary barbels brown, rictal barbel brownish white. Fins hyaline; dark chromatophores scattered over all fins, except pelvic fin. In juvenile specimens about 40 mm SL or less (Fig. 11), flank, dorsum and head side light brownish yellow with small black dots irregularly arranged.

Distribution. *Cambeva rotundipinna* is known from two close localities in the Rio da Paca, a tributary of the Rio Jangada, Rio Iguaçu drainage, Rio Paraná basin, at about 1000 m asl (Fig. 5).

Etymology. From the Latin rotundus (rounded) and pinna (fin or wing), an allusion to the rounded fins of this new species.

Discussion

Phylogenetic analyses indicated that the four species here described found at high altitudes do not form a monophyletic group, thus not supporting a common origin, but, in contrast, supported relationships of RISE species at different nodes of the phylogenetic tree (Fig. 1). On the other hand, all the four species are supported as members of the *Cambeva* beta1-clade, with *C. galactica*, endemic to eastern RISE as the sister group to all other species of this clade (Fig. 1). In *C. galactica*, there are six pectoral-fin rays, characteristic that never occurs in other species *Cambeva* beta1-clade (i.e. seven or eight pectoral-fin rays) but is present in species with a more basal position within the more inclusive *Cambeva* beta-clade, such as *C. flavopicta* Costa, Feltrin & Katz, 2020, *C. naipi*, and *C. taroba*, possibly consisting of a plesiomorphic feature for the *Cambeva* beta1-clade.

The position of *C. atrobrunnea*, *C. luteoreticulata*, and *C. rotundipinna* in a phylogenetic tree section with low resolution does not allow us to have an accurate view of their closest relationships. They appear as basal taxa relative to an apical clade including *C. barbosae*, *C. diabola*, *C. castroi* and *C. davisi* (Fig. 1, hereafter *Cambeva davisi* group), which are separated from each other by short genetic distances. Whereas *C. atrobrunnea*, *C. luteoreticulata*, and *C. rotundipinna* were only found at higher altitudes, between about 970 and 1,015 m asl, species of the *C. davisi* group were found at low and middle altitudes, between about 15 and 850 m asl (e.g. Bockmann et al. 2004; Costa et al. 2021b). The phylogenetic position of *C. atrobrunnea*, *C. luteoreticulata*, and *C. rotundipinna* relative to the *C. davisi* group suggests an older origin of those species living in higher altitudes. However, more robust phylogenies with the inclusion of yet undescribed species from neighbouring regions and species already described but not available for molecular analyses are necessary to infer the evolutionary history of the *Cambeva* beta-clade in southern Brazilian mountains.

Cambeva rotundipinna appears weakly supported as the sister group to *C. stawiarski*, but it was not possible to identify morphological characters corroborating relationships between these two species when examining comparative material of *C. stawiarski* (UFRJ 11846, 4 ex., 25°30'33"S, 53°40'59"W; UFRJ 11847, 3 ex., UFRJ 13620, 1 ex (C&S), 25°30'33"S, 53°40'59"W; UFRJ 11850, 2 ex. (C&S), about 25°40'S, 52°00'W; UFRJ 13541, 3 ex., 26°20'11"S, 49°32'18"W). However, the mesethmoidal region of *C. rotundipinna* bears great similarity to that illustrated for *C. cauim*, a species difficult to distinguish from *C. stawiarski* by external morphological characters and probably closely related to it (Reis et al. 2021). *Cambeva cauim*, also endemic to the Iguaçu River drainage (Reis et al. 2021), was not included in our phylogenetic analysis and specimens were not available for morphological examination, but its detailed original description allows us to make accurate comparisons. In both *C. rotundipinna* and *C. cauim*, the mesethmoid is wide in its anterior portion, with the cornua being subtriangular and slightly curved posteriorly, narrowing abruptly at its ends, and the autopalatine has a pronounced expansion on its postero-medial margin (Fig. 4J; Reis et al. 2021: fig. 2A), besides the urohyal having relatively short lateral and posterior processes (Fig. 4L; Reis et al. 2021: fig. 7A). *Cambeva rotundipinna* is easily distinguished from *C. cauim* by having a rounded caudal fin (vs. emarginate) and 15–17 dorsal procurrent caudal-fin rays (vs. 30 or 31), in addition to the unique diagnostic character states above described for *C. rotundipinna*. *Cambeva atrobrunnea* was weakly supported as sister to the *Cambeva davisi* group. However, in the present comparative morphological analysis, it was not possible to find any evidence of a close relationship between *C. atrobrunnea* and species of this group.

Acknowledgements

We are grateful to Luis E. H. Sebben and family for help and support during field studies and to Diego da Silva for sending comparative material. Special thanks are also due to M. Petrungaro, L. I. Chaves, B. R. dos Santos, M. R. dos Santos, and L. Neves for technical assistance in the fish collection. This study was funded by Conselho Nacional de Desenvolvimento Científico e Tecnológico (CNPq; grant 304755/2020-6 to WJEMC) and Fundação Carlos Chagas Filho de Amparo à Pesquisa do Estado do Rio de Janeiro (FAPERJ; grant E-26/201.213/2021 to WJEMC, E-26/203.524/2023 to JLOM; and E-26/202.005/2020 to AMK). This study was also supported by CAPES (Finance Code 001) through the Programa de Pós-Graduação em: Biodiversidade e Biologia Evolutiva/UFRJ and Genética/UFRJ.

References

Ab'Saber A (2007) Os domínios de natureza no Brasil: potencialidades paisagísticas. Ateliê Editoral, São Paulo, 4th edn., 160 pp.

Aguiar RG, Guimarães EC, Brito PS, Santos JP, Katz AM, Dias LJBS, Carvalho-Costa LF, Ottoni FP (2022) A new species of *Knodus* (Characiformes: Characidae), with deep genetic divergence, from the Mearim and Munim river basins, Northeastern Brazil, and evidence for hidden diversity in adjacent river basins. Neotropical Ichthyology 20: e210173. https://doi.org/10.1590/1982-0224-2021-0173

Arratia G, Huaquin L (1995) Morphology of the lateral line system and of the skin of diplomystid and certain primitive loricarioid catfishes and systematic and ecological considerations. Bonner Zoologische Monographien 36: 1–110.

Arratia G, Menu Marque S (1984) New catfishes of the genus *Trichomycterus* from the high Andes of South America (Pisces, Siluriformes)

with remarks on distribution and ecology. Zoologische Jahrbücher 111: 493–520.

Barros LC, Santos U, Cioffi MDB, Dergam JA (2015) Evolutionary divergence among Oligosarcus spp. Ostariophysi, Characidae from the São Francisco and Doce River Basins: Oligosarcus solitarius Menezes, 1987 shows the highest rates of chromosomal evolution in the Neotropical region. Zebrafish 12: 102–110. https://doi.org/10.1089/zeb.2014.1030

Bockmann FA, Casatti L, de Pinna MCC (2004) A new species of trichomycterid catfish from the Rio Paranapanema basin, southeastern Brazil (Teleostei: Siluriformes), with comments on the phylogeny of the family. Ichthyological Exploration of Freshwaters 15: 225–242.

Bockmann FA, Sazima I (2004) *Trichomycterus maracaya*, a new catfish from the upper rio Paraná, southeastern Brazil (Siluriformes: Trichomycteridae), with notes on the *T. brasiliensis* species-complex. Neotropical Ichthyology 2: 61–74. https://doi.org/10.1590/S1679-62252004000200003

Castellanos-Morales CA (2008) *Trichomycterus uisae*: a new species of hypogean catfish (Siluriformes: Trichomycteridae) from the northeastern Andean Cordillera of Colombia. Neotropical Ichthyology 6: 307–314. https://doi.org/10.1590/S1679-62252008000300003

Castellanos-Morales CA (2018) A new species of cave catfish, genus *Trichomycterus* (Siluriformes: Trichomycteridae), from the Magdalena River system, Cordillera Oriental, Colombia. Biota Colombiana 19 (Sup. 1): 117–130. https://doi.org/10.21068/c2018.v19s1a10

Chenna R, Sugawara H, Koike T, Lopez R, Gibson TJ, Higgins DG, Thompson JD (2003) Multiple sequence alignment with the Clustal series of programs. Nucleic Acids Research 31: 3497–3500. https://doi.org/10.1093/nar/gkg500

Costa WJEM (1992) Description de huit nouvelles espèces du genre *Trichomycterus* (Siluriformes: Trichomycteridae), du Brésil oriental. Revue Française d'Aquariologie et Herpetologie 18: 101–110.

Costa WJEM (2021) Comparative osteology, phylogeny and classification of the eastern South American catfish genus *Trichomycterus* (Siluriformes: Trichomycteridae). Taxonomy 1: 160–191. https://doi.org/10.3390/taxonomy1020013

Costa WJEM, Amorim PF, Aranha GN (2014) Species limits and DNA barcodes in *Nematolebias*, a genus of seasonal killifishes threatened with extinction from the Atlantic Forest of south-eastern Brazil, with description of a new species (Teleostei: Rivulidae). Ichthyological Exploration of Freshwaters 24: 225–36.

Costa WJEM, Katz AM, Mattos JLO, Amorim PF, Mesquita BO, Vilardo PJ, Barbosa MA (2020a) Historical review and redescription of three poorly known species of the catfish genus *Trichomycterus* from south-eastern Brazil (Siluriformes: Trichomycteridae). Journal of Natural History 53: 2905–2928. https://doi.org/10.1080/00222933.2020.1752406

Costa WJEM, Henschel E, Katz AM (2020b) Multigene phylogeny reveals convergent evolution in small interstitial catfishes from the Amazon and Atlantic forests (Siluriformes: Trichomycteridae). Zoologica Scripta 49: 159–173. https://doi.org/10.1111/zsc.12403

Costa WJEM, Feltrin CRM, Katz AM (2021a) Field inventory reveals high diversity of new species of mountain catfishes, genus *Cambeva* (Siluriformes: Trichomycteridae), in south-eastern Serra Geral, southern Brazil. Zoosystema 43: 659–690. https://doi.org/10.5252/zoosystema2021v43a28

Costa WJEM, Feltrin CRM, Katz AM (2021b) Filling distribution gaps: Two new species of the catfish genus *Cambeva* from southern Brazilian Atlantic Forest (Siluriformes: Trichomycteridae). Zoosystematics and Evolution 97: 147–159. https://doi.org/10.3897/zse.97.61006

Costa WJEM, Abilhoa V, Dalcin RH, Katz AM (2022) A new catfish species of the genus *Cambeva* (Siluriformes: Trichomycteridae) from the Rio Iguaçu drainage, southern Brazil, with a remarkable unique colour pattern. Journal of Fish Biology 101: 69–76. https://doi.org/10.1111/jfb.15071

Costa WJEM, Feltrin CRM, Mattos JLM, Amorim PFA, Katz AM (2023a) Phylogenetic relationships of new taxa support repeated pelvic fin loss in mountain catfishes from southern Brazil (Siluriformes: Trichomycteridae). Zoologischer Anzeiger 305: 82–90. https://doi.org/10.1016/j.jcz.2023.06.003

Costa WJEM, Feltrin CRM, Mattos JLO, Dalcin RH, Abilhoa V, Katz AM (2023b) Morpho-Molecular Discordance? Re-Approaching Systematics of *Cambeva* (Siluriformes: Trichomycteridae) from the Guaratuba-Babitonga-Itapocu Area, Southern Brazil. Fishes 8: 63. https://doi.org/10.3390/fishes8020063

Cramer CA, Bonatto SL, Reis RE (2011) Molecular phylogeny of the Neoplecostominae and Hypoptopomatinae (Siluriformes: Loricariidae) using multiple genes. Molecular Phylogenetics and Evolution 59: 43–52. https://doi.org/10.1016/j.ympev.2011.01.002

Davis JI, Nixon KC (1992) Populations, genetic variation, and the delimitation of phylogenetic species. Systematic Biology 41: 421–435. https://doi.org/10.1093/sysbio/41.4.421

DeSalle R, Egan MG, Siddall M (2005) The unholy trinity: taxonomy, species delimitation and DNA barcoding. Philophical Transactions of the Royal Society B, 360: 1905–1916. https://doi.org/10.1098/rstb.2005.1722

de Pinna MCC (1992) Trichomycterus castroi, a new species of trichomycterid catfish from the Rio Iguaçu of southeastern Brazil (Teleostei, Siluriformes). Ichthyological Exploration of Freshwaters 3: 89–95.

DoNascimiento C, Prada-Pedreros S, Guerrero-Kommritz J (2014) A new catfish species of the genus *Trichomycterus* (Siluriformes: Trichomycteridae) from the río Orinoco versant of Páramo de Cruz Verde, Eastern Cordillera of Colombia. Neotropical Ichthyology 12: 717–728. https://doi.org/10.1590/1982-0224-20140005

Donin LM, Ferrer J, Carvalho TP (2022) Uncertainties and risks in delimiting species of *Cambeva* (Siluriformes: Trichomycteridae) with single-locus methods and geographically restricted data. Neotropical Ichthyology 20: e220019. https://doi.org/10.1590/1982-0224-2022-0019

dos Reis RB, Ferrer J, da Graça WJ (2021) A new species of *Cambeva* (Siluriformes, Trichomycteridae) from the Rio Iguaçu basin, Paraná state, Brazil and redescription of *Cambeva stawiarski* (Miranda Ribeiro 1968). Journal of Fish Biology 96: 350–363. https://doi.org/10.1111/jfb.14204

dos Reis RB, Frota A, Fabrin TMC, da Graça WJ (2019) A new species of Cambeva (Siluriformes, Trichomycteridae) from the Rio Ivaí basin, upper Rio Paraná basin, Paraná state, Brazil. Journal of Fish Biology 96: 350–363. https://doi.org/10.1111/jfb.14906

Fernández L, Contrera G, Bize JA (2023) New species of *Trichomycterus* (Siluriformes: Trichomycteridae) from wetlands of high elevation of Argentina, with notes on the *T. alterus* species-complex. Ichthyology & Herpetology 111: 456–466. https://doi.org/10.1643/i2022074

Fernández L, Liotta J (2016) *Silvinichthys pachonensis*, a new catfish from high altitude, with a key to the species of the genus (Siluriformes: Trichomycteridae). Ichthyological Exploration of Freshwaters 27: 375–383.

Fernández L, de Pinna MCC (2005) A phreatic catfish of the genus Silvinichthys from southern South America (Teleostei, Siluriformes, Trichomycteridae). Copeia 2005: 100–108. https://doi.org/10.1643/CI-03-158R2

Fernández L, Schaefer SA (2003) *Trichomycterus yuska*, a new species from high elevations of Argentina (Siluriformes: Trichomycteridae). Ichthyological Exploration of Freshwaters 14: 353–360.

Fernández L, Vari RP (2012) New species of *Trichomycterus* (Teleostei: Siluriformes) from the Andean Cordillera of Argentina and the second record of the genus in thermal waters. Copeia 2012: 631–636. https://doi.org/10.1643/CI-12-035

Ferrer J, Malabarba LR (2011) A new *Trichomycterus* lacking pelvic fins and pelvic girdle with a very restricted range in Southern Brazil (Siluriformes: Trichomycteridae). Zootaxa 2912: 59–67. https://doi.org/10.11646/zootaxa.2912.1.5

Hardman M, Page LM (2003) Phylogenetic relationships among bullhead catfishes of the genus *Ameiurus* (Siluriformes: Ictaluridae). Copeia 2003: 20–33. https://doi.org/10.1643/0045-8511(2003)003[0020:PRABCO]2.0.CO;2

Haseman JD (1911) Some new species of fishes from the Rio Iguassú. Annals of the Carnegie Museum 7: 374–387 [+ pls. 48, 50, 58, 73–83] https://doi.org/10.5962/p.167633

Hoang DT, Chernomor O, von Haeseler A, Minh BQ, Vinh LS (2018) UFBoot2: Improving the ultrafast bootstrap approximation. Molecular Biology and Evolution 35: 518–522. https://doi.org/10.1093/molbev/msx281

Katz AM, Barbosa MA, Mattos JLO, Costa WJEM (2018) Multigene analysis of the catfish genus *Trichomycterus* and description of a new South American trichomycterine genus (Siluriformes, Trichomycteridae). Zoosystematics and Evolution 94: 557–566. https://doi.org/10.3897/zse.94.29872

Kimura M (1980) A simple method for estimating evolutionary rates of base substitutions through comparative studies of nucleotide sequences. Journal of Molecular Evolution 16: 111–120. https://doi.org/10.1007/BF01731581

Kubicek KM (2022) Developmental osteology of *Ictalurus punctatus* and *Noturus gyrinus* (Siluriformes: Ictaluridae) with a discussion of siluriform bone homologies. Vertebrate Zoology 72: 661–727. https://doi.org/10.3897/vz.72.e85144

Lanfear R, Frandsen PB, Wright AM, Senfeld T, Calcott B (2017) PartitionFinder 2: New methods for selecting partitioned models of evolution for molecular and morphological phylogenetic analyses. Molecular Biology and Evolution 34: 772–773. https://doi.org/10.1093/molbev/msw260

Mesa LM, Lasso CA, Ochoa LE, DoNascimiento C (2018) *Trichomycterus rosablanca* (Siluriformes, Trichomycteridae) a new species of hipogeancatfish from the Colombian Andes. Biota Colombiana 19 (Sup. 1): 95–116. https://doi.org/10.21068/c2018.v19s1a09

Minh BQ, Schmidt HA, Chernomor O, Schrempf D, Woodhams MD, von Haeseler A, Lanfear R (2020) IQ-TREE 2: New models and efficient methods for phylogenetic inference in the genomic era. Molecular Biology and Evolution 37: 1530–1534. https://doi.org/10.1093/molbev/msaa015

Miranda-Ribeiro P de (1968) Notas para o estudo dos Pygidiidae brasileiros VIII. Boletim do Museu Nacional 265: 1–3.

Myers N, Mittermeir RA, Mittermeir CG, da Fonseca GAB, Kent J (2000) Biodiversity hotspots for conservation priorities. Nature 403: 853–858. https://doi.org/10.1038/35002501

Ochoa LE, Roxo FF, DoNascimiento C, Sabaj MH, Datovo A, Alfaro M, Oliveira C (2017a) Multilocus analysis of the catfish family Trichomycteridae (Teleostei: Ostariophysi: Siluriformes) supporting a monophyletic Trichomycterinae. Molecular Phylogenetics and Evolution 115: 71e81. https://doi.org/10.1016/j.ympev.2017.07.007

Ochoa LE, Silva GSC, Costa e Silva GJ, Oliveira C, Datovo A (2017b) New species of *Trichomycterus* (Siluriformes: Trichomycteridae) lacking pelvic fins from Paranapanema basin, southeastern Brazil. Zootaxa 4319: 550–560. https://doi.org/10.11646/zootaxa.4319.3.7

Rahbek C, Gote NJ, Colwell RK, Entstninger GL, Rangel Thiago FLVB, Graves GR (2007) Predicting continental-scale patterns of bird species richness with spatially explicit models Proceedings of the Royal Society B 274: 165–174. https://doi.org/10.1098/rspb.2006.3700

Rahbek C, Borregaard MK, Antonelli A, Colwell RK, Holt BG, Nogues-Bravo D, Rasmussen CMØ, Richardson K, Rosing MT, Whittaker RJ, Fjeldså J (2019) Building mountain biodiversity: geological and evolutionary processes. Science 365: 1114–1119. https://doi.org/10.1126/science.aax0151

Rambaut A, Drummond AJ, Xie D, Baele G, Suchard MA (2018) Posterior summarization in Bayesian phylogenetics using Tracer 1.7. Systematic Biology 67: 901–904 . https://doi.org/10.1093/sysbio/syy032

Suchard MA, Lemey P, Baele G, Ayres DL, Drummond AJ, Rambaut A (2018) Bayesian phylogenetic and phylodynamic data integration using BEAST 1.10. Virus Evolution 4: 1–5. https://doi.org/10.1093/ve/vey016

Swofford DL (2003) PAUP*, Phylogenetic Analysis Using Parsimony (*and Other Methods). Version 4, Sinauer Associates, Sunderland, Massachusetts.

Tamura K, Stecher G, Kumar S (2021) MEGA11: Molecular Evolutionary Genetics Analysis Version 11. Molecular Biology and Evolution 38: 3022–3027. https://doi.org/10.1093/molbev/msab120

Taylor WR, Van Dyke GC (1985) Revised procedures for staining and clearing small fishes and other vertebrates for bone and cartilage study. Cybium 9: 107–119.

Unmack PJ, Bennin AP, Habi EM, Victoriano PF, Johnson JB (2009) Impact of ocean barriers, topography, and glaciation on the phylogeography of the catfish Trichomycterus areolatus (Teleostei: Trichomycteridae) in Chile. Biological Journal of the Linnean Society 97: 876–892. https://doi.org/10.1111/j.1095-8312.2009.01224.x

Valenciennes A (1832) Nouvelles observations sur le Capitan de Bogota, *Eremophilus mutisii*. In: Humboldt, A. & Bonpland, A. Recueil d'observations de Zoologie et d'Anatomie Comparée, faites dans l'Ocean Atlantique, dans l'interieur du Nouveau Continent et dans la Mer du Sud pendant les annés 1799, 1800, 1801, 1802 et 1803, deuxième volume. Observations de Zoologie et d'Anatomie comparée, 341–348.

Villa-Verde L, Lazzarotto H, Lima SQM (2012) A new glanapterygine catfish of the genus *Listrura* (Siluriformes: Trichomycteridae) from southeastern Brazil, corroborated by morphological and molecular data. Neotropical Ichthyology 10: 527–538. https://doi.org/10.1590/S1679-62252012000300005

Ward RD, Zemlak TS, Innes BH, Last PR, Hebert PD (2005) DNA barcoding Australia's fish species. Philosophical Transactions of the Royal Society of London B Biological Sciences 360: 1847–1857. https://doi.org/10.1098/rstb.2005.1716

Wosiacki WB, de Pinna M (2008a) *Trichomycterus igobi*, a new catfish species from the rio Iguaçu drainage: The largest head in Trichomycteridae (Siluriformes: Trichomycteridae). Neotropical Ichthyology 6: 17–23. https://doi.org/10.1590/S1679-62252008000100003

Wosiacki WB, de Pinna M (2008b) A new species of the Neotropical catfish genus Trichomycterus (Siluriformes: Trichomycteridae) representing a new body shape for the family. Copeia 2008: 273–278. https://doi.org/10.1643/CI-06-237

Wosiacki WB, Garavello JC (2004) Five new species of Trichomycterus from the Iguaçu (rio Paraná Basin), southern Brazil (Siluriformes: Trichomycteridae). Ichthyological Exploration of Freshwaters 15: 1–16.